UNIVERSIDADE FEDERAL DE LAVRAS

RÔMULO MARÇAL GANDIA

THE INFLUENCE OF FLOW PATTERN AND HOPPER ANGLE ON STATIC AND DYNAMIC PRESSURES IN SLENDER SILOS

LAVRAS - MG
2023

RÔMULO MARÇAL GANDIA

THE INFLUENCE OF FLOW PATTERN AND HOPPER ANGLE ON STATIC AND DYNAMIC PRESSURES IN SLENDER SILOS

Trabalho de Conclusão de Curso apresentada à Universidade Federal de Lavras, como parte das exigências do Programa de Graduação em Engenharia Civil, para a obtenção do título de bacharel.

Orientador
Dr. Wisner Coimbra de Paula

Coorientador
Dr. Francisco Carlos Gomes

LAVRAS - MG

2023

RÔMULO MARÇAL GANDIA

THE INFLUENCE OF FLOW PATTERN AND HOPPER ANGLE ON STATIC AND DYNAMIC PRESSURES IN SLENDER SILOS

A INFLUÊNCIA DO PADRÃO DE FLUXO E DO ÂNGULO DA TREMONHA NAS PRESSÕES ESTÁTICAS E DINÂMICAS EM SILOS ESBELTOS

Trabalho de Conclusão de Curso apresentada à Universidade Federal de Lavras, como parte das exigências do Programa de Graduação em Engenharia Civil, para a obtenção do título de bacharel.

APROVADO em 07 de fevereiro de 2023

Dr. Wisner Coimbra de Paula	Universidade Federal de Lavras
Dr. Francisco Carlos Gomes	Universidade Federal de Lavras
Ma. Simone Mancini	Centro Universitário de Lavras

Documento assinado digitalmente
gov.br WISNER COIMBRA DE PAULA
Data: 27/02/2023 09:18:03-0300
Verifique em https://verificador.iti.br

Dr. Wisner Coimbra de Paula
Orientador

Dr. Francisco Carlos Gomes
Coorientador

Documento assinado digitalmente
gov.br FRANCISCO CARLOS GOMES
Data: 27/02/2023 12:17:01-0300
Verifique em https://verificador.iti.br

LAVRAS - MG
2023

Dedico este trabalho à minha família, minha base, meu tudo.
Albany Lourenço G. Gandia, meu pai, que me ***estrutura****,*
Marta Lúcia P. M. Gandia, minha mãe, que me ***ilumina****,*
Rodrigo M. Gandia, meu irmão a quem me ***espelho*** *e*
Ísis W. S. Gandia, minha filha a quem me ***dedico****.*

AGRADECIMENTOS

Agradeço a Deus, presente em todos os momentos. Onipresente nos momentos mais difíceis.

Sobre ombro de Gigantes, a metáfora dos anões em latim: *nanos gigantum humeris incidentes*. Expressa o significado de "descobrir a verdade a partir das descobertas anteriores".

Agradeço aos meus, primeiramente, grandes amigos e professores, Dr. Francisco Carlos Gomes, Dr. Wisner Coimbra de Paula por estarem comigo desde o início dessa jornada e por terem me auxiliado nos estudos.

Aos meus grandes amigos que contribuíram diretamente nesse trabalho a equipe de trabalho do Centro de Processamento e Pesquisa dos Produtos Armazenados.

A todos que sempre estiveram comigo, meus amigos, meus parentes, meus professores. Todos que de alguma maneira serviram de guia, mentor e conselheiro em minha vida profissional e pessoal.

A Universidade Federal de Lavras, minha casa. Nessa casa, a todos que indiretamente fez ser possível, ao pessoal da limpeza, pessoal da vigilância, aos técnicos, aos servidores, ao pessoal da secretaria, meu muito obrigado.

Por fim, reforço o maior agradecimento a meus pais pelo incentivo, por possibilitar, por acreditar, pelo carinho, pela dedicação e pelo sacrifício durante toda a minha vida na busca por conhecimento. A meu irmão por me incentivar e ser meu exemplo de vida.

ABSTRACT

The experimental station for pilot-scale silo pressure measurements was the basis for data collection in this article. Results were reported for pressures and flows analysis using a free-flowing product at our experimental station. Five different hopper angles were tested by filling the silo, and observing a static phase followed by complete discharge. The results show that: Hopper angle influences the normal pressures in the silo wall; Silos with transition flow have no pattern results; Pressures are proportional to the increase and decrease of β°during filling and discharge; Mechanical arches vary according to the hopper angles completely modifying the behavior of static and dynamic pressures. Some parameters exceeded those calculated by the standard: friction pressure and lateral pressure ratio. Many aspects remain poorly understood and still need to be studied experimentally for a better understanding of the patterns and theories regarding pressures, stored product, hopper angle and flow in silos.

Keywords: Experimental station for silo pressures; slender silo; friction and normal pressures; free-flowing product; flow pattern.

RESUMO

A estação experimental para medições de pressão de silo em escala piloto foi a base para a coleta de dados neste artigo. Os resultados foram relatados para análises de pressões e fluxos usando um produto de fluxo livre na estação experimental. Foram analisados cinco diferentes ângulos de tremonha. O silo foi carregado até a altura de interesse, analisado a fase estática e depois descarregando completamente. Os resultados mostram que: O ângulo da tremonha influencia as pressões normais na parede do silo; Silos com fluxo de transição não têm resultados de padrão; As pressões são proporcionais ao aumento e diminuição de β° durante o enchimento e a descarga; Os arcos mecânicos variam de acordo com os ângulos da tremonha modificando completamente o comportamento das pressões estáticas e dinâmicas. Alguns parâmetros ultrapassaram os calculados pela norma: pressão de atrito e razão de pressão lateral. Muitos aspectos permanecem pouco compreendidos e ainda precisam ser estudados experimentalmente para uma melhor compreensão dos padrões e teorias sobre pressões, material armazenado, ângulo de tremonha e fluxo em silos.

Palavras-chave: Estação experimental para pressões de silos; silo esbelto; pressões normais e de atrito; produto de fluxo livre; padrão de fluxo.

FIGURE LIST

Firts Part

Second Part

SUMMARY

FIRST PART

General Summary

The main objective of this work is to understand the actions, mainly the pressures on the walls, in slender cylindrical silos. For this, such silos were experimentally studied.

The article, “The influence of flow pattern and hopper angle on static and dynamic pressures in slender silos”, will be submitted to the scientific journal Powder Technology, presents static and dynamic experimental results of horizontal and frictional pressures, coefficient K, analyzes the maximum pressures, always comparing with Eurocode, analyzing the types of flows and five different angles of hoppers using h/d ratio 3.6.

The installation used for the experimental tests is based on the model by Pieper and Schütz (1980), providing the basis for the DIN 1055-6 standard (DIN, 2005). The experimental station is modular and proved to be versatile, allowing numerous configuretion possibilities due to its instrumentation and structural independence.

1. INTRODUCTION

The agricultural sector in Brazil grows considerably. The estimated grain production for the 2021/2022 harvest is 284.4 million tons (CONAB - COMPANHIA NACIONAL DE ABASTECIMENTO, 2022). In 2019, Brazil has the static capacity of 177.7 million tons of grains, with 86.6 million (49%) being in silos (DPE - DIRETORIA DE PESQUISA E COORDENAÇÃO AGROPECUÁRIA, 2019).

However, despite the aforementioned data, Brazil Brazil had the first standard approved for silo projects in December 2022, ABNT NBR 17066 - Silos metálicos de chapas corrugadas (ABNT NBR 17066 - Corrugated sheet metal silos).

The study of the behavior of products stored in silos dates back to 1895 by Janssen (JANSSEN, 1895). Since then, other theories have been developed (WALKER, 1967) (WALTERS, 1973a, 1973b) (JENIKE; JOHANSON; CARSON, 1973a) supporting international standards (CEN, 2006; DIN, 2005).

The main causes failures and collapses in silos refer to design errors; on pressures (normal and friction, on the wall and in the hopper) of the product stored in the structure; excess moisture in the stored product (causing unexpected pressure behaviors); product discharge step (maximum pressures in the silo, generally in the silo-hopper transition); discharge eccentricity; temperature variation in the product due to silo location and imperfections in the structural material.

The pilot scale test station proposed by Pieper and Schütz in 1980 (PIEPER; SCHÜTZ, 1980) supported DIN 1055-6: Basis of design and actions on structures – Part 6 (DIN, 2005) allows obtaining numerous variables that directly influence in the behavior of pressures in the silo.

The experimental model of real-scale silos provides proximity to real values, enabling confidence in the data and making it possible to understand the pressures in the silos. In the world, the number of full-scale experimental silo stations for investigating pressures is relatively small due to the cost of construction, instrumentation, and operations.

Therefore, this work aims evaluate the influence of flow pattern and hopper angle on static and dynamic pressures in slender silos using a free flow stored product (maize).

2. THEORETICAL REFERENCE

2.1. Silos

The first tall silos were built from 1870 onwards, a time when calculators believed that stored products behaved like liquids, designing the structures to resist pressures equivalent to hydrostatics.

According to Roberts (1884 apud PALMA, 2005), after carrying out tests on small-scale models, he found that grains differed in their behavior in relation to liquids. In their observations, it was found that the vertical pressures on the silo walls increased linearly with height up to a certain point, after which the behavior changed and was no longer proportional to height.

In this way, the aforementioned author concluded that a portion of the weight of the stored product was transferred to the walls through product-wall friction. Thus, the pressures on the bottom and walls, in the lowest part of a silo, are lower than those exerted by a liquid (Figure 1).

Figure 1 - Difference between liquids and solids in pressure distribution.

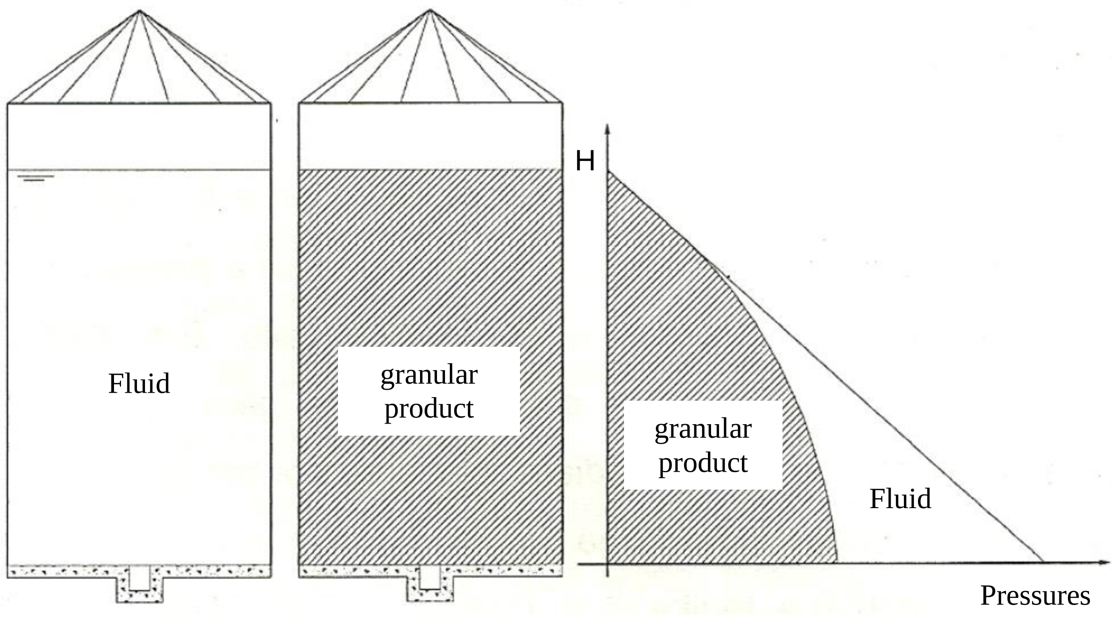

Source: CALIL; CHEUNG (2007).

Janssen (1895) pioneered the establishment of a theory for calculating the pressures occurring in silos. His study was based on square wooden silo in which, through the analysis of an infinitesimal part of the stored product, pressures were obtained via balance of forces. However, this study considered the condition of static filling and, it is known today, that in conditions of filling and discharge of the silo, higher pressures occur.

As stated, the characteristics of granular and powdery products are different from liquids, making the design of silos more complex in relation to continuous flows and as economic and safe structures and, for this to occur, it is essential that loads are not underestimated or overrated.

During the processing of products stored in silos with gravity discharge, it is essential that the filling and discharge of the silos occur in an effective and efficient way, requiring knowledge of the relevant physical and flow properties of the stored products (MILANI, 1993).

The first step in the design of flow and structures of vertical silos is the determination of the physical properties of stored products, using the most severe conditions that can occur in the silo (CALIL; NASCIMENTO; ARAUJO, 1997).

The physical properties of the stored products must be known or determined to carry out a project, for this, the method and equipment developed by Jenike (SCHWEDES, 1983) makes this determination possible. Therefore, the main measurable properties of granular and powdery products are (GAYLORD; GAYLORD, 1984):

- angle of repose
- internal friction angle (φ_i)
- effective angle of internal friction (φ_e)
- angle and coefficient of friction with the wall (φ_w)
- specific weight depending on the state of consolidation
- product moisture (ϫ)
- granulometry.

The behavior of pressures in a silo is influenced by the flow pattern, and the two parameters that directly influence it are the hopper angle and the friction angle between the stored product and the hopper wall. There are two possible flow patterns, mass flow and funnel flow. (CEN, 2006), directly influencing the magnitude and distribution of forces acting on the silo (JENIKE; JOHANSON; CARSON, 1973a). A third flow pattern, transition flow, is characterized by a distinct change in flow at a position that depends on the filling height (BENINK, 1989).

The discharge of the stored product by gravity can occur as shown in the Figure 2.

Figure 2 - Main types of flow.

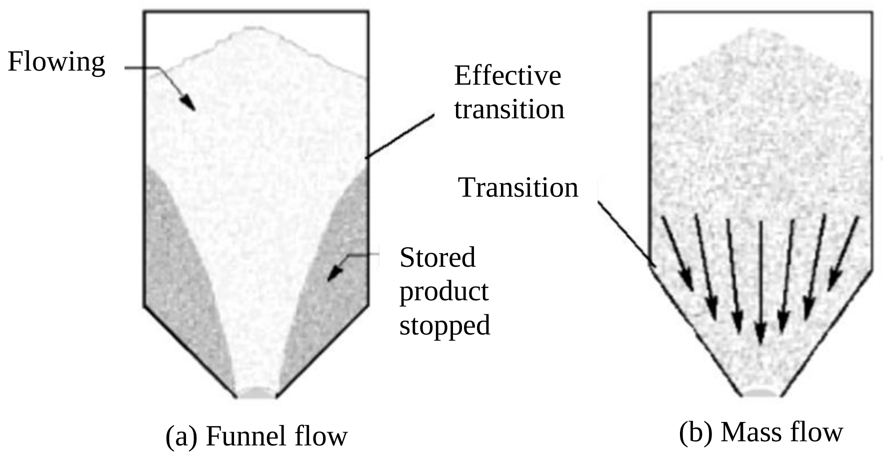

Source:Palma (2005).

To determine the type of flow, the European international standard (CEN, 2006) determines through graphs that involve some variables (Figure 3). The graphs predict the type of flow as a function of the angle of the hopper or the coefficient of friction of the stored product with the wall, the slope of the hopper walls and their geometry (generally conical or pyramidal, concentric).

Figure 3 - Obtaining the type of flow.

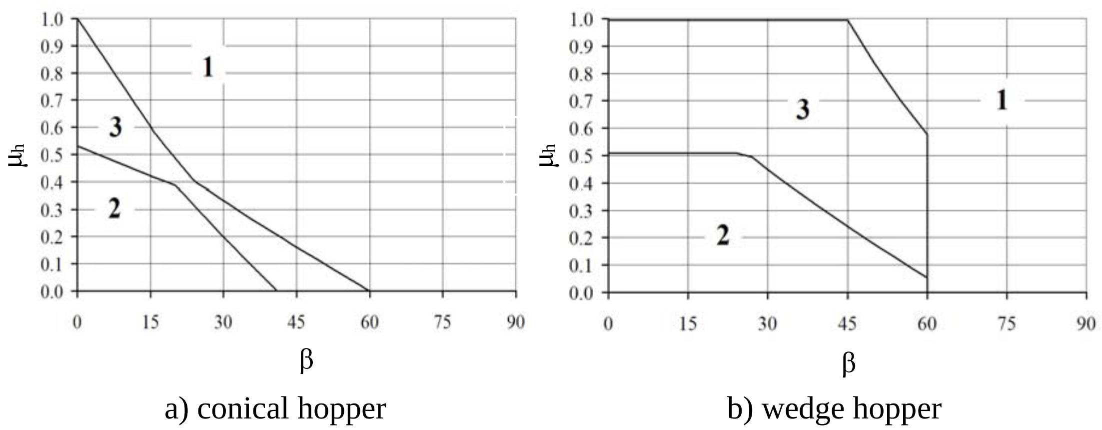

Where:

1 = Funnel Flow;
2 = Mass flow;
3 = Mass flow or funnel;
β = Hopper inclination angle;
μ_h = Friction coefficient.

Source:Adaptado from EN 1991-4 (2006).

The hopper geometry (angle and size of the outlet opening) and the type of product stored (contact surface, roughness) used in the construction of the silo hopper define the type of flow, allowing to evaluate the behavior of the product inside the silo. Therefore, according to the characteristics of the products, various types of hoppers are used and chosen.

The prediction of the type of flow based on the friction angle of the product with the silo wall ($ø_w$) and on the internal friction angle of the stored product ($ø_e$) to define the hopper angle (α) has been a matter of investigation.

2.2. Pressures on the walls and bottom of slender silos

Many variables involved in this estimation pressures on the walls and bottom of slender silos, one statement is certain: the pressures exerted on the silo walls are directly related to the type of flow at the time of silo discharge.

The estimation of pressures in silos for funnel flow presents more uncertainties and variability than for mass flow (CALIL, 1985). Due to the complexity of the laws that govern the mechanical behavior of stored products directly associated with the accuracy in the prediction of flow types, there is much to study about the geometric shapes of silos, filling and discharge configurations and types of hoppers (AYUGA, 2008; DOGANGUN et al., 2009; GANDIA et al., 2021d; NIELSEN, 2008).

The stored product exerts pressure on the silo structure: walls – horizontal and friction pressure; hopper – normal and friction pressure; transition (silo-hopper) vertical pressure. On the silo wall perpendicular forces act, causing horizontal pressures (p_h), and parallel forces due to friction of the product with the wall, causing friction pressures (p_w). In the silo transition (silo-hopper) vertical forces occur, causing the so-called vertical pressures (p_v). In the hopper, the normal forces and friction forces act from the vertical pressures that were decomposed into normal and tangential pressures to the hopper wall, represented by p_n and p_t, respectively (Figure 4).

Figure 4 – Distribution of pressures in the silo.

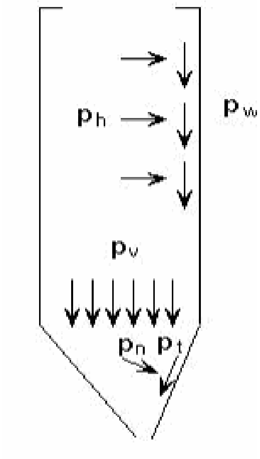

Source: Palma (2005).

The silo dynamics is defined by the silo filling, static phase and discharge. Pressures during filling present divergent discharge behaviors, these different situations occur the formation of maximum pressures (pressure peaks) due to the rapid change of state of the stored product, from passive to active (GANDIA et al., 2021c; PALMA, 2005; RUIZ; COUTO; AGUADO, 2012) (Figure 5). The percentage of increase in pressures (overpressures) in relation to the filling phase is still the subject of discussions and research.

Figure 5 – Stress field in silos (mass flow).

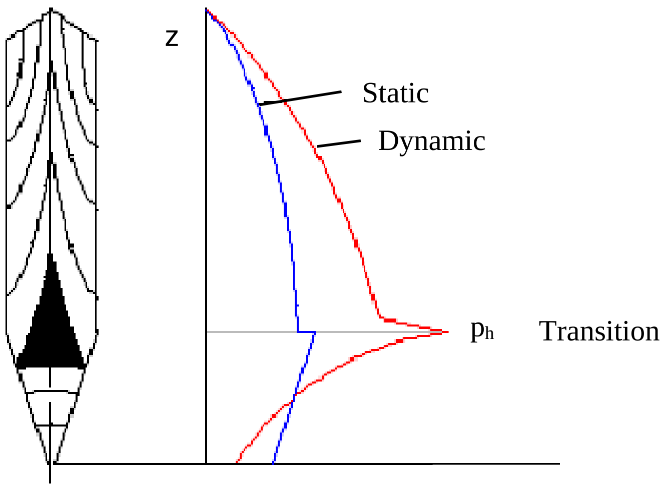

Source: Palma (2005).

At the beginning of discharge, the highest pressures in the silo occur, therefore, special attention is required. These pressures are located in the transition zone (silo/hopper), these overpressures usually occur within the first 10 seconds after the start of discharge (RUIZ; COUTO; AGUADO, 2012), however, due to the slenderness of the silo and the inclination of the hopper, this peak can exceed 10 seconds (GANDIA et al., 2021c).

The transition region that occurs the change from passive to active state, mentioned above, is called “switch”. This "peak" of pressure provided by the change of stress states has been studied by several researchers (JANSSEN, 1895; JENIKE; JOHANSON; CARSON, 1973a, 1973b; WALKER, 1967; WALTERS, 1973b, 1973a) developing theories and procedures, generating base for many studies.

3. GENERAL CONSIDERATIONS

The storage of agricultural products presents great national and international importance in terms of inventory control, logistics, quality, and safety. Therefore, the storage of products in silos is increasing because we have many gaps due to the properties of the stored products and the dynamic structure that is the silo. Therefore, the importance of the experimental study is remarkable for presenting realistic and accurate answers.

This work is composed of two parts. The first part is a synthetic and generalized approach to the motivation and theoretical basis of the studies. The second part presents one article with theoretical and methodological depth followed by the results and conclusions.

The second part showed that with this the test station is possible to determine normal and friction pressure related with consolidation; time of occurrence of maximum silo pressure after discharge starts; relationships between different pressure, consolidation, discharge time by flow type, influence of flow type on discharge pressures and other variables and relationships.

REFERENCES

AGRICULTURA Y GANADERIA DE CASTILLA Y LEÓN. **TABLAS DE LA COSECHA DE MAÍZ 2020 EN CASTILLA Y LEÓN**. [s.l: s.n.]. Disponível em: <https://agriculturaganaderia.jcyl.es/web/jcyl/AgriculturaGanaderia/es/Plantilla100Detalle/1246464862173/Noticia/1284998741023/Recurso>.

ANSI - AMERICAN SOCIETY OF AGRICULTURAL AND BIOLOGICAL ENGINEERS. **Loads Exerted by Free-Flowing Grain on Bins. ANSI/ASAE**: S433.1 JAN2019. St Joseph: [s.n.].

AUSTRALIAN STANDARD. AS 3774. **Loads on bulk containers. AS 3774 Supplement 1 (1997)**. Sydney: [s.n.].

AYUGA, F. et al. Discharge and the Eccentricity of the Hopper Influence on the Silo Wall Pressures. **Journal of Engineering Mechanics**, v. 127, n. 10, p. 1067–1074, 2001.

AYUGA, F. et al. Experimental tests to validate numerical models in silos design. **2006 ASABE Annual International Meeting**, v. 0300, n. 06, 2006.

AYUGA, F. Some unresolved problems in the design of steel cylindrical silos. In: CHEN, J.F., TENG, J. G. (Ed.). . **Structures and Granular Solids: From Scientific Principles to Engineering Applications**. Boca Raton, USA: CRC Press-Taylor & Francis Group, 2008. p. 123–133.

BARLETTA, D.; POLETTO, M. A device for the measurement of the horizontal to vertical stress ratio in powders. **Granular Matter**, v. 15, n. 4, p. 487–497, 2013.

BARLETTA, D.; POLETTO, M. A new split cell for the measurement of the horizontal to vertical stress ratio of powders. **Powder Technology**, v. 351, p. 273–281, 2019.

BENINK, E. J. **Flow and stress analysis of cohesionless bulk materials in silos related to codes**. [s.l.] University of Twente, 1989.

BROWN, C. J.; LAHLOUH, E. H.; ROTTER, J. M. Experiments on a square planform steel silo. **Chemical Engineering Science**, v. 55, n. 20, p. 4399–4413, 2000.

BROWN, C. J.; NIELSEN, J. **Silos: Fundamentals of theory, behaviour and design**. London: [s.n.].

BUTTERFIELD, R. A theoretical study of the pressures developed in a silo containing single-size particles in a regular packing. **International Journal of Rock Mechanics and Mining Sciences and**, v. 6, n. 2, p. 227–238, 1969.

BYWALSKI, C.; KAMIŃSKI, M. A case study of the collapse of the over-chamber reinforced concrete ceiling of a meal silo. **Engineering Structures**, v. 192, n. March, p. 103–112, 2019.

CALIL, C.; PALMA, G.; CHEUNG, A. B. Failure Modes of Cylindrical Corrugated Steel Silos in Brazil. **Bulk solids handling**, v. 29, n. 6, p. 346, 2009.

CALIL, J. C. Cargas para o dimensionamento de silos. **JORNADAS SUL-AMERICANAS DE ENGENHARIA ESTRUTURAL**, v. 23, p. 1359–1379, 1985.

CALIL, J. C. **Recomendações de Fluxo e de Cargas para o Projeto de Silos Verticais**. [s.l.] Tese de Livre Docência. EESC - USP, 1990.

CALIL, J. C.; CHEUNG, A. B. **Silos: pressões, fluxo, recomendações para o projeto e exemplo de cálculo**. São Carlos: [s.n.].

CALIL, J. C.; NASCIMENTO, J. W. B. DO; ARAUJO, E. C. **Silos Metálicos Multicelulares**. [s.l.] Serviço Gráfico - EESC / USP, 1997.

CEN. **EN 1991-4:2006. Eurocode 1: Actions on Structures. Part 4: Silos and Tanks**. Brussels: [s.n.].

CHEN, J. F. et al. Correlation between the flow pattern and wall pressures in a full scale experimental silo. **Engineering Structures**, v. 29, n. 9, p. 2308–2320, 2007.

CHEN, Y. et al. Static pressure distribution characteristics of powders stored in silos. **Chemical Engineering Research and Design**, v. 154, n. 2014, p. 1–10, 2020.

CHEUNG, A. B. **MODELO ESTOCÁSTICO DE PRESSÕES DE PRODUTOS ARMAZENADOS PARA A ESTIMATIVA DA CONFIABILIDADE ESTRUTURAL DE SILOS ESBELTOS**. [s.l.] Universidade de São Paulo, 2007.

CONAB - COMPANHIA NACIONAL DE ABASTECIMENTO. **Acompanhamento da safra brasileira de grãossafra 2021/22, n. 4 quarto levantamento**. Brasilia: [s.n.]. Disponível em: <https://www.conab.gov.br/component/k2/item/download/40788_0ee9dd05157257045355d00863c854b0>.

COUTO, A. et al. Measuring pressures in a slender cylindrical silo for storing maize. Filling, static state and discharge with different material flow rates and comparison with Eurocode 1 part 4. **Computers and Electronics in Agriculture**, v. 96, p. 40–56, 2013.

COUTO, A.; RUIZ, A.; AGUADO, P. J. Design and instrumentation of a mid-size test station for measuring static and dynamic pressures in silos under different conditions - Part I: Description. **Computers and Electronics in Agriculture**, v. 85, p. 164–173, 2012.

COUTO, A.; RUIZ, A.; AGUADO, P. J. Experimental study of the pressures exerted by wheat stored in slender cylindrical silos, varying the flow rate of material during discharge. Comparison with Eurocode 1 part 4. **Powder Technology**, v. 237, p. 450–467, 2013.

DE PAULA, W. C. et al. **AVALIAÇÃO DAS PRESSÕES VERTICAIS NO FUNDO PLANO DE UM SILO ESBELTO**. XLIX Congresso Brasileiro de Engenharia Agrícola - CONBEA 2020. **Anais**...2020

DESHMUKH, O. S. et al. Ring Shear Tester as an in-vitro testing tool to study oral processing of comminuted potato chips. **Food Research International**, v. 123, n. November 2018, p. 208–216, 2019.

DEUTSH, G. P.; SCHMIDT, L. C. Pressures on Silo Walls. **Developments in Geotechnical Engineering**, v. 39, n. C, p. 125–138, 1985.

DIN. **DIN 1055-6: Basis of design and actions on structures – Part 6: design 623 loads for buildings and loads in silo bins**. Berlin, Verlaz: 2005

DOGANGUN, A. et al. Cause of damage and failures in silo structures. **Journal of Performance of Constructed Facilities**, v. 23, n. 2, p. 65–71, 2009.

DPE - DIRETORIA DE PESQUISA E COORDENAÇÃO AGROPECUÁRIA. **IBGE - Pesquisa de Estoques 2º semestre de 2019**. [s.l: s.n.].

DRUCKER, D. C.; PRAGER, W. Soil mechanics and plastic analysis or limit design. **Quart. Appl. Math**, v. 10, n. 2, p. 157–165, 1952.

FANK, M. Z. et al. Vertical pressures and compressive friction force in a large silo. **Engenharia Agricola**, v. 38, n. 4, p. 498–503, 2018.

GALLEGO, E. et al. SIMULATIONS OF GRANULAR FLOW IN SILOS WITH DIFFERENT FINITE ELEMENT PROGRAMS: ANSYS VS. SILO. **Transactions of the ASABE**, v. 53, n. 3, p. 819–829, 2010.

GALLEGO, E.; RUIZ, A.; AGUADO, P. J. Simulation of silo filling and discharge using ANSYS and comparison with experimental data. **Computers and Electronics in Agriculture**, v. 118, p. 281–289, 2015.

GANDIA, R. M. et al. Static and dynamic pressure measurements of maize grain in silos under different conditions. **Biosystems Engineering**, v. 209, p. 180–199, 2021a.

GANDIA, R. M. et al. Influence of specific weight and wall friction coefficient on normal pressures in silos using the Finite Element Method. **Revista Engenharia na Agricultura - Reveng**, v. 29, p. 192–203, 2021b.

GANDIA, R. M. et al. Evaluation of pressures in slender silos varying hopper angle and silo slenderness. **Powder Technology**, v. 394, p. 478–495, 2021c.

GANDIA, R. M. et al. Evaluation of pressures in slender silos varying hopper angle and silo slenderness. **Powder Technology**, v. 394, p. 478–495, 2021d.

GANDIA, R. M. et al. Static and dynamic pressure measurements of maize grain in silos under different conditions. **Biosystems Engineering**, v. 209, p. 180–199, 2021e.

GAYLORD, E. D.; GAYLORD, C. . **Design of steel bins for storage of bulk solids**. New Jersey: Prentice-Hall: [s.n.].

GOMES, F. C.; CALIL, J. C. Estudo Teórico experimental das ações em silos horizontais. **Cadernos de Engenharia de Estruturas**, v. 7, p. 33–62, 2005.

GONZÁLEZ-MONTELLANO, C. et al. Validation and experimental calibration of 3D discrete element models for the simulation of the discharge flow in silos. **Chemical Engineering Science**, v. 66, n. 21, p. 5116–5126, 2011.

GOODEY, R. J.; BROWN, C. J.; ROTTER, J. M. Predicted patterns of filling pressures in thin-walled square silos. **Engineering Structures**, v. 28, n. 1, p. 109–119, 2006.

GUAITA, M.; COUTO, A.; AYUGA, F. Numerical simulation of wall pressure during discharge of granular material from cylindrical silos with eccentric hoppers. **Biosystems Engineering**, v. 85, n. 1, p. 101–109, 2003.

GUTIÉRREZ, G. et al. Silo collapse under granular discharge. **Physical Review Letters**, v. 114, n. 1, p. 5–9, 2015.

HÄRTL, J. et al. The influence of a cone-in-cone insert on flow pattern and wall pressure in a full-scale silo. **Chemical Engineering Research and Design**, v. 86, n. 4, p. 370–378, 2008.

HOLST, J. M. F. G. et al. Numerical Modeling of Silo Filling. I: Continuum Analyses. **Journal of Engineering Mechanics**, v. 125, n. 1, p. 94–103, 1999.

INTERNACIONAL ORGANIZATION FOR STANDARDIZATION. **ISO 11697:2012. Bases for design of strutures - Loads due to bulk materials**. [s.l: s.n.].

JA. B LVIN. Analytical Evaluation of Pressures of Granular Materials on Silo Walls. **Powder Technology**, v. 4, n. 5, p. 280, 1971.

JANSSEN, H. A. Versuche uber getreidedruck in silozellen. **Z. Ver. Dtsch. Ing**, v. 39, n. 35, p. 1045–1049, 1895.

JENIKE, A. . **Storage and Flow of Bulk Solids Bull. 123**. USA: University of Utah, 1964.

JENIKE, A. W.; JOHANSON, J. R.; CARSON, J. W. Bin loads—part 3: mass-flow bins. **Journal of Manufacturing Science and Engineering, Transactions of the ASME**, v. 95, n. 1, p. 6–12, 1973a.

JENIKE, A. W.; JOHANSON, J. R.; CARSON, J. W. Bin Loads—Part 4: Funnel-Flow Bins. **Journal of engineering for Industry**, v. 95, p. 13–20, 1973b.

LOPES NETO, J. P.; NASCIMENTO, J. W. B. DO; FANK, M. Z. Forças verticais e de atrito em silos cilíndricos com fundo plano. **Revista Brasileira de Engenharia Agrícola e Ambiental**, v. 18, n. 6, p. 652–657, 2014.

MILANI, A. P. **Determinação das propriedades de produtos armazenados para o projeto de pressões e fluxo em silos**. [s.l.] Universidade de São Paulo, 1993.

MINISTÉRIO DA AGRICULTURA PESCA Y ALIMENTACIÓN. **Avances de superficies y producciones agrícolas. Diciembre 2020**. [s.l: s.n.].

MOYA, M. et al. MECHANICAL PROPERTIES OF GRANULAR AGRICULTURAL MATERIALS. **Transactions of the ASABE**, v. 45, n. 5, p. 1569–1577, 2002.

NASCIMENTO, J. W. B. DO; LOPES NETO, J. P.; MONTROSS, M. D. Horizontal pressures in cylindrical metal silos and comparison with different international standards. **Engenharia Agricola**, v. 4, p. 601–611, 2013.

NIELSEN, J. Pressures from flowing granular solids in silos. **Philosophical Transactions of the Royal Society A: Mathematical, Physical and Engineering**

Sciences, v. 356, n. 1747, p. 2667–2684, 1998.

NIELSEN, J. From silo phenomena to load models. In: CHEN, J. F.; TENG, J. G. (Eds.). . **Structures and Granular Solids: From Scientific Principles to Engineering Applications**. Boca Raton, USA: CRC Press-Taylor & Francis Group, 2008. p. 49–57.

NIELSEN, J.; ASKEGAARD, V. Scale errors in model tests on granular media with special reference to silo models. **Powder Technology**, v. 16, n. 1, p. 123–130, 1977.

PALMA, G. **PRESSÕES E FLUXO EM SILOS ESBELTOS (h/d≥1,5)**. [s.l.] Universidade de São Paulo, 2005.

PARDIKAR, K.; ZAHID, S.; WASSGREN, C. Quantitative comparison of experimental and Mohr-Coulomb finite element method simulation flow characteristics from quasi two-dimensional flat-bottomed bins. **Powder Technology**, v. 367, p. 689–702, 2020.

PIEPER, K.; SCHÜTZ, M. **Bericht Über das Forschungsvorhaben - Norm-Mess-Silo für Schüttguteigenschaften**. [s.l.] Technische Universität Braunschweig, 1980.

RAMÍREZ, A. et al. Analysis of Measurements Obtained by Plate-type Pressure Cells Having a Recess - DEM Simulation. **Bulk Solids & Powder – Science & Technology**, v. 4, n. January, 2009.

RAMÍREZ, A.; NIELSEN, J.; AYUGA, F. On the use of plate-type normal pressure cells in silos. Part 1: Calibration and evaluation. **Computers and Electronics in Agriculture**, v. 71, n. 1, p. 71–76, 2010a.

RAMÍREZ, A.; NIELSEN, J.; AYUGA, F. Pressure measurements in steel silos with eccentric hoppers. **Powder Technology**, v. 201, n. 1, p. 7–20, 2010b.

RAVENET, J. **RAVENET, J. Silo: deformaciones, falhas, explosiones, prevencion de. Barcelona, Ed. Tecnicos Associados**Barcelona, 1983.

ROTTER, J. M.; BROWN, C. J.; LAHLOUH, E. H. Patterns of wall pressure on filling a square planform steel silo. **Engineering Structures**, v. 24, n. 2, p. 135–150, 2002.

RUIZ, A.; COUTO, A.; AGUADO, P. J. Design and instrumentation of a mid-size test station for measuring static and dynamic pressures in silos under different conditions - Part II: Construction and validation. **Computers and Electronics in Agriculture**, v. 85, p. 174–187, 2012.

SADOWSKI, A. J.; MICHAEL ROTTER, J.; NIELSEN, J. A theory for pressures in cylindrical silos under concentric mixed flow. **Chemical Engineering Science**, v. 223, p. 115748, 2020.

SADOWSKI, A. J.; ROTTER, J. M. Structural Behavior of Thin-Walled Metal Silos Subject to Different Flow Channel Sizes under Eccentric Discharge Pressures. **Journal of Structural Engineering**, v. 138, n. 7, p. 922–931, 2012.

SALEHI, H. et al. Temperature and Time Consolidation Effect on the Bulk Flow Properties and Arching Tendency of a Detergent Powder. **Chemical Engineering and**

Technology, v. 43, n. 1, p. 150–156, 2020.

SCHULZE, D. Silos – Design Variants and Special Types. **Bulk Solids Handling**, v. 16, n. 2, 1996.

SCHURICHT, T.; FURLL, C.; EENSTAD, G. G. Full scale silo tests and numerical simulations of the „cone in cone" concept for mass flow. In: **Handbook of Powder Technology**. [s.l.] Elsevier Science BV, 2001. v. 10p. 175–180.

SCHWAB, C. V et al. WHEAT LOADS AND VERTICAL PRESSURE. v. 37, n. 5, p. 1613–1619, 1994.

SCHWEDES, J. Evolution of bulk solids technology since 1974. **Bulk solids handling**, v. 3, n. 1, 1983.

SONG, C. Y.; TENG, J. G. Buckling of circular steel silos subject to code-specified eccentric discharge pressures. **Engineering Structures**, v. 25, n. 11, p. 1397–1417, 2003.

SUN, W. et al. Multi-scale experimental study on filling and discharge of squat silos with aboveground conveying channels. **Journal of Stored Products Research**, v. 88, p. 101679, 2020.

SUN, Y.; WANG, Y. Collapse reasons analysis of a large steel silo. **Advanced Materials Research**, v. 368–373, p. 647–650, 2012.

TEIXEIRA, L. G.; GOMES, F. C. **Determinação dos ângulos de atrito interno, efetivo e do ângulo de atrito com a parede do produto café utilizando a máquina de cisalhamento TSG 70-140**. Congresso Brasileiro de Engenharia Agrícola. **Anais**...Goiânia: 2003

TENG, B. J. PLASTIC COLLAPSE AT LAP JOINTS IN PRESSURIZED CYLINDERS UNDER AXIAL LOAD. v. 120, n. 1, p. 23–45, 1994.

TENG, J. G.; LIN, X. Fabrication of small models of large cylinders with extensive welding for buckling experiments. **Thin-Walled Structures**, v. 43, n. 7, p. 1091–1114, 2005.

TENG, J. G.; ROTTER, J. M. Plastic collapse of restrained steel silo hoppers. **Journal of Constructional Steel Research**, v. 14, n. 2, p. 139–158, 1989.

TENG, J. G.; ZHAO, Y.; LAM, L. Techniques for buckling experiments on steel silo transition junctions. **Thin-Walled Structures**, v. 39, n. 8, p. 685–707, 2001.

TENG, J.; ROTTER, J. M. Collapse Behavior and Strength of Steel Silo Transition Junctions. Part I: Collapse Mechanics. **Journal of Structural Engineering**, v. 117, n. 12, p. 3587–3604, 1991.

WALKER, D. An approximate theory for pressures and arching in hoppers. **Chemical Engineering Science**, v. 22, n. 3, p. 486, 1967.

WALTERS, J. K. A theoretical analysis of stresses in axially-symmetric hoppers and bunkers. **Chemical Engineering Science**, v. 28, n. 3, p. 779–789, 1973a.

WALTERS, J. K. A theoretical analysis of stresses in silos with vertical walls. **ChemicalEngineering Science**, v. 28, p. 13–21, 1973b.

WENZEL, F. Pressure behavior in double cylindrical silos. **Journal of Manufacturing Science and Engineering, Transactions of the ASME**, v. 95, n. 1, p. 97–100, 1973.

WÓJCIK, M. et al. Full-scale experiments on wheat flow in steel silo composed of corrugated walls and columns. **Powder Technology**, v. 311, p. 537–555, 2017.

WÓJCIK, M.; TEJCHMAN, J.; ENSTAD, G. G. Confined granular flow in silos with inserts - Full-scale experiments. **Powder Technology**, v. 222, p. 15–36, 2012.

WPMPS. **Standart Shear Testing Technique for Particulate Solids Using the Jenike Shear Cell“**. England: [s.n.].

YÁÑEZ, Á. C.; FEMÁNDEZ, M. G.; LÓPEZ, P. V. ANÁLISIS DE LA DISTRIBUCIÓN DE PRESIONES ESTÁTICAS EN SILOS CILÍNDRICOS CON TOLVA EXCÉNTRICA MEDIANTE EL M. E. F. INFLUENCIA DE LA EXCENTRICIDAD Y COMPARACIÓN CON EL EUROCÓDIGO 1. **Informes de la Construcción**, v. 52, n. 472, p. 17–27, 2001.

ZEGZULKA, J. The angle of internal friction as a measure of work loss in granular material flow. **Powder Technology**, v. 233, p. 347–353, 2013.

ZHAO, Q.; JOFRIET, J. C. Structural loads on bunker silo walls: Numerical study. **Journal of Agricultural Engineering Research**, v. 51, n. C, p. 1–13, 1992.

ZHAO, Y.; TENG, J. G. Buckling experiments on steel silo transition junctions. II: Finite element modeling. **Journal of Constructional Steel Research**, v. 60, n. 12, p. 1803–1823, 2004.

ZHONG, Z.; OOI, J. Y.; ROTTER, J. M. The sensitivity of silo flow and wall stresses to filling method. **Engineering Structures**, v. 23, n. 7, p. 756–767, 2001.

SECOND PART

Article 1 – The influence of flow pattern and hopper angle on static and dynamic pressures in slender silos - Powder Technology journal (preliminary version)

The article was submitted to the Powder Technology journal (ISSN 0032-5910). The journal has the qualis A1 and JCR 5.134.

The influence of flow pattern and hopper angle on static and dynamic pressures in slender silos

Rômulo Marçal Gandia[1,2*], Francisco Carlos Gomes[1], Wisner Coimbra de Paula[1], Pedro José Aguado Rodriguez[2]

[1]Federal University of Lavras (Brazil), Agricultural Engineering Department
[2]University of León (Spain), Department of Engineering and Agricultural Sciences

ABSTRACT

Our experimental station for pilot-scale silo pressure measurements was the basis for data collection in this article. Results were reported for pressures and flows analysis using a free-flowing product at our experimental station. Five different hopper angles were tested by filling the silo, and observing a static phase followed by complete discharge. Our results show that: Hopper angle influences the normal pressures in the silo wall; Silos with transition flow have no pattern results; Pressures are proportional to the increase and decrease of β°during filling and discharge; Mechanical arches vary according to the hopper angles completely modifying the behavior of static and dynamic pressures. Some parameters exceeded those calculated by the standard: friction pressure and lateral pressure ratio. Many aspects remain poorly understood and still need to be studied experimentally for a better understanding of the patterns and theories regarding pressures, stored product, hopper angle and flow in silos.

KEYWORDS: experimental station for silo pressures, slender silo, friction and normal pressures, free-flowing product, flow pattern.

Nomenclature

Symbols

Ø: Angle of internal friction, degrees

A: Plan cross-sectional area of vertical walled segment, m^2

d_i: Internal cylinder diameter, m.

$F_{h(1,12)u,t}$: Force in tension load cell positioned on the upper part of the spring set - rings 1 to 12, at time t, kN

$F_{h(1,12)d,t}$: Force in tension load cell positioned on the lower part of the spring set - rings 1 to 12, at time t, kN

$F_{w(1,12)r,t}$: Force in tension load cell positioned on the right side of the ring support - rings 1 to 12, at time t, kN

$F_{w(1,12)l,t}$: Force in tension load cell positioned on the left side of the ring support - rings 1 to 12, at time t, kN

$F_{vtr,t}$: Force in tension load cell positioned on the right side of the hopper support, at time t, kN

$F_{vtl,t}$: Force in tension load cell positioned on left side of the hopper support, at time t, kN

$F_{vbr,t}$: Force on shear beam load cell positioned at the base of the right pillar, time t, kN

$F_{vbl,t}$: Force on shear beam load cell positioned at the base of the left pillar, time t, kN

h: Ring height, m.

K: Characteristic value of lateral pressure ratio

$P_{ntr,t}$: Normal pressure on the right hopper wall next to the silo–hopper transition, time t, kPa

$P_{ntl,t}$: Normal pressure on left hopper wall next to the silo–hopper transition, time t, kPa

$P_{nir,t}$: Normal pressure on right hopper wall between the silo–hopper transition and outlet, time t, kPa

$P_{nil,t}$: Normal pressure on left hopper wall between the silo–hopper transition and outlet, time t, kPa

$P_{nitr,t}$: Normal pressure on right hopper wall between the silo–hopper transition and outlet, near transition, time t, kPa

$P_{nitl,t}$: Normal pressure for left hopper wall between the silo–hopper transition and the outlet, near transition, time t, kPa

$P_{nior,t}$: Normal pressure on right hopper wall between the silo–hopper transition and outlet, near outlet, time t, kPa

$P_{niol,t}$: Normal pressure on left hopper wall between the silo–hopper transition and outlet, near outlet, time t, kPa

$P_{nor,t}$: Normal pressure on the right hopper wall next to silo outlet, time t, kPa

$P_{nol,t}$: Normal pressure for the hopper wall on the left-hand side next to silo outlet, time t, kPa

$P_{h(1,12),t}$: Normal pressure on cylinder wall from the tension load cells positioned on spring set - rings 1 to 12, time t, kPa

$P_{w(1,12),t}$: Friction pressure for the cylinder wall from the tension load cells positioned on ring supports - rings 1 to 12, time t, kPa

$P_{vt,t}$: Vertical stress of product at the silo–hopper transition from the tension load cells positioned on the hopper support, time t, kPa

$P_{v(1,4),t}$: Vertical stress of product at the silo–hopper transition obtained from the pressure cells (flat bottom), time t, kPa

$W_{,t}$: Weight of stored product, time t, kN

W_{hto}: Weight of stored product between the outlet and the silo–hopper transition, zero in the case of the flat bottom, kN

V_{ih}: Internal hopper volume, m^3

V_{ic}: Internal cylinder volume, m^3

r_i: Internal cylinder radius, m.

γ: Bulk unit weight

1. Introduction

The study of the behavior of products stored in silos is dated from 1895 by Janssen [1]. Since then, other theories have been developed [2] [3,4] [5] supporting international standards [6,7]. Jenike [8] developed a device, internationally known, capable of determining the flow properties of stored products (Jenike Shear Tester), later improved by a group (Working Party on the Mechanics of Particulate Solids) of the European Federal of Chemical Engineers, renamed to "*Standart Shear Testing Technique for Particulate Solids Using the Jenike Shear Cell*" [9]. This device, in addition to supporting international standards, is capable of obtaining reliable parameters for calculating projects in silos.

The main reason that the study in silos is broad and complex is due to the behavior of the stored products. The laws that govern the mechanical behavior is presents complexities, therefore, many aspects remain poorly understood [10–12]. Consequently, to study actions, pressures and flows in silos, it is necessary to understand the structure, the product inside the structure and the interaction between them.

Brazil is a continental country with a favorable climate and relief for agricultural production. Therefore, the agricultural sector in Brazil is growing. The estimated grain production for the 2021/2022 harvest is 284.4 million tons [13]. Of this total, 87 million tons (25%) correspond to maize. Motivated by the future market, storage control, logistics or cooperatives, most agricultural products are stored. In 1980, the Brazilian storage capacity was 40.45 million tons of grain. In less than 4 decades (2019), Brazil more than quadrupled its static capacity (177.7 million tons of grain), with 86.6 million (49%) being in silos [14]. In addition, maize is also a leading product in the international market, for example, in Spain, with a production of 4.1 million tons

[15], with León being the Spanish province with the highest production, 0.9 million [16].

In addition to the complexity of the mechanical behavior of maize and its derivatives, both have the highest load magnifying factor coefficient due to geometric unevenness (C_{op} = 1,0 e 0,9 for animal feed mix and maize respectively), Table E.1 – Particulate solids properties, Eurocode 1, part 4 [7]. This coefficient is directly related to obtaining the pressures in the silos [7]. Experimental studies aid in the responses to these irregular stored products, quantifying pressure values throughout the silo.

The complexity of studying pressures in silos is due to the behavior being different from hydrostatic pressures, in other words, the stored product in silos presents friction pressures on the wall that increase according to the storage height [17].

The causes of silo failures and collapses are driven by several reasons. A review of some studies showed that the design error [18,19] and pressures stand out. The pressure (normal and friction) occurs in the silo wall and in the hopper. These pressures are static [10,19] (during filling and storage period) and dynamic (at the time of discharge) [10,19–22] and are exerted by the stored product in the structure.

The pressures in the silo are related by flow pattern that is directly influenced by the stored product and the hopper geometry. There are two possible flow patterns, mass flow [5] and funnel flow [23], and also has a flow transition zone: transition flow, that is characterized by a distinct change in flow in a position that depends on the filling height [24]. These flow patterns directly influence the magnitude and distribution of forces acting across the silo. The hopper angle and the wall friction coefficient are the two most influential parameters [7,8,25,26]. [7,8,25]However, flow pressure is still poorly understood [17,27–29].

Faced with the several causes that lead to failures in the silo structure include the pressures (normal and friction, on the wall and hopper) exerted by the stored product in the structure [10,19] and the product discharge (maximum pressures in the silo, usually at the silo-hopper transition) [10,19–22]. Reinforcing the need for studies involving pressures, especially at discharge. The study of friction pressures in relation to silo height has been little studied.

A pilot-scale test station proposed by Pieper and Schütz in 1980 [30] supported DIN 1055-6: *Basis of design and actions on structures – Part 6* [6] allows obtaining numerous variables that directly influence the behavior of pressures in the silo [31,32], of which: use of any product as long as the maximum diameter of the product is less than 1.7 centimeters (to be allowed values proportional to the real scale) [30,33]; three walls with different roughness (varying the coefficient of friction between the product and the wall); twelve height/diameter ratios; 8 bottoms (1 flat bottom, 4 concentric hoppers (α: 75 to 30o) and 3 100% eccentric hoppers with (α: 75 to 45o) and other possible test procedure variables. The test station was developed and studied at the University from Sao Paulo [34] later, in partnership, it was calibrated and studies are currently being developed at the Federal University of Lavras [35].

The experimental model of real-scale silos provides proximity to real values, enabling confidence in the data and enabling the understanding of pressures in the silos. In the world, the number of real-scale experimental silo stations for investigating pressures is relatively small. [35–46] due to the cost of construction, instrumentation and operations. In addition, the scale factor is extremely important for reliable data. [33]. Furthermore, the study of experimental pressures in silo allows the advancement of numerical studies as a form of validation and comparisons in order to make the models reliable.

Therefore, the aim of the present study was to elucidate the relationship involving the hopper angle, flow pattern and the pressures in slender cylindrical silos, obtaining normal and frictional pressures on the wall and pressures on the hopper wall during filling, static phase and discharge of the stored product.

2. Material and methods

2.1. General description of the installation

The silo test station corresponds to the pilot scale [33], that is, if the appropriate proportions between the stored product and the internal diameter of the silo are used, the values of the loads and pressures correspond to the real scale. The station consists of a pilot silo (fully instrumented), a storage silo (store the product stored during the tests) and a bucket elevator (transport between the silos). All the measuring cells of the pilot silo are connected in the acquisition system data controlled by a portable computer (Figure 1).

Figure 6. Pilot silo station and instrumentation.

2.1.2. Geometry of the experimental pilot silo

The pilot test silo is cylindrical and metallic. The cylinder is 6 meters high and 0.7 meters in internal diameter. The cylinder is segmented into 12 structurally independent rings, allowing to obtain the forces in each division. The pilot silo is classified as slender [6,7,25]. As only 5 rings were used in this work, the Figure 2 shows the location of the measurement cells up to the height of 2.50 m (5 rings).

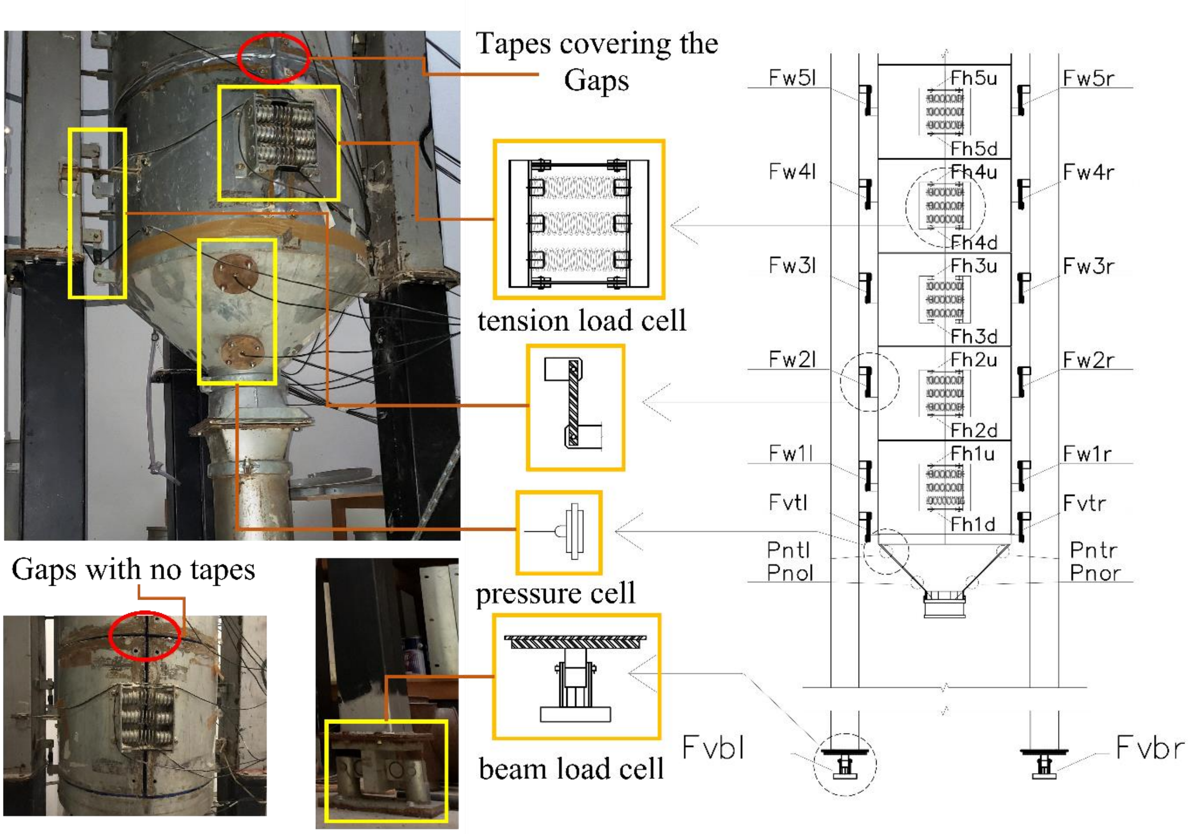

Figure 7. Instrumentation and measurement cells for loads and pressures of the pilot silo.

2.2. Measuring vertical forces

The pilot silo is supported by two support pillars supporting pillars with shear beam load cells at its bases (Figure 2), enabling the measurement of the weight of the stored product.

The vertical forces responsible for measuring the friction pressure of the cylinder wall and vertical stress in the stored product at the transition were measured by tension load cell located on each support pillar along the height of the pilot silo vertically supporting each ring and the bottom (Figure 2).

2.3. Measuring horizontal forces and normal pressures

Measurements in the hopper were conducted using pressure cells (Figure 2). To measure normal wall pressures, a vertical generatrix was located on the cylinder wall, along which 12 pairs of readings were taken at different heights using a tension load cell, each pair were responsible for providing normal pressure at each ring (Figure 2).

The arrangement of the measuring cells influences the data obtained [47,48]. The pressure cells have a gap of 2.5 mm in the radius between the cell and the hopper structure. In addition, the cell is 10 mm high (part that is internal to the silo), the wall thickness of the hoppers is exactly 10 mm, ensuring quality in data collection. Each ring was spaced 5 mm apart (vertical distance) and had a gap of 5 mm in the opening (horizontal distance).

2.4. Calculation of parameters

In this section, the station parameters are presented briefly. The most detailed explanation of the parameters is in Gandia et al. (2021) [49].

Normal wall pressures (Ph)

$$\mathbf{Ph(1,5),t} = \frac{\mathbf{Fh(1{,}5)u{,}t + Fh(1{,}5)d{,}t}}{\mathbf{hr.0.32759}}, \text{ equation (1)}$$

- 0.32759: constant value obtained with $d_i = 0.685$ m.

Frictional wall pressures (Pw)

$$\mathbf{Pw(1,5),t} = \frac{\boldsymbol{Fw(1{,}5)r{,}t + Fw(1{,}5)l{,}t}}{\mathbf{\pi.di.hr}}, \text{ equation (2)}$$

Weight of stored product (W)

$$\mathrm{W,t} = \mathrm{Fvbr,t} + \mathrm{Fvbr,t} \quad \text{equation (3):}$$

Vertical stress in the stored solid at the transition (P_{vt})

$$\mathbf{Pvt,t} = \frac{\mathbf{Fvtr{,}t + Fvtl{,}t - Whto}}{\mathbf{A}} \text{ equation (4):}$$

$$\mathbf{Whto} = \mathbf{Vi}\boldsymbol{h} * \boldsymbol{\gamma}$$ equation (5):

Wall friction coefficient (μ)

$$\mu(1{,}5) = \frac{\mathrm{Pw}(1{,}12)}{\mathrm{Ph}(1{,}12)}$$ equation (6):

Lateral pressure ratio (K)

$$\mathrm{K,t} = \frac{\mathrm{Ph}(1{,}5),t}{\mathrm{Pv}(1{,}5),t}$$ equation (7):

Specific weight of stored product (γ)

$$\gamma = \frac{W}{\mathrm{Vih+Vic}}$$ equation (8)

2.5. Description of the tests

2.5.1. Properties of the stored product

The product used to conduct the tests in the pilot silo was maize with a minimum purity of 97%. The physical, mechanical and flow properties of maize were obtained following the methodology of Jenike Shear Test [9] which conforms to Eurocode 1, part 4 [7]. The values obtained were (lower and upper limits):

- specific weight (kN/m^3): 7.52 – 7.83
- angle of repose, 31.3° - 37.1;
- cohesion (kPa): 0.241 – 1.084;
- steel wall friction angle: 7.37° – 9.02°;
- steel wall friction coefficient: 0.13 - 0.16;
- internal friction angle: 19° - 29°;
- humidity, 10.62%.

2.5.2. Test settings

Using the granular product described above, 30 tests were performed. The tests were conducted with concentric filling. The 30 tests were divided into five configurations (Figure 3) with six repetitions each. The configurations have different hopper inclinations, where: β = 15 ° (β15°); β = 30 ° (β30°); β = 45 ° (β45°); β = 60 ° (β60°) and β = 90 °, named a flat bottom (FlatB).

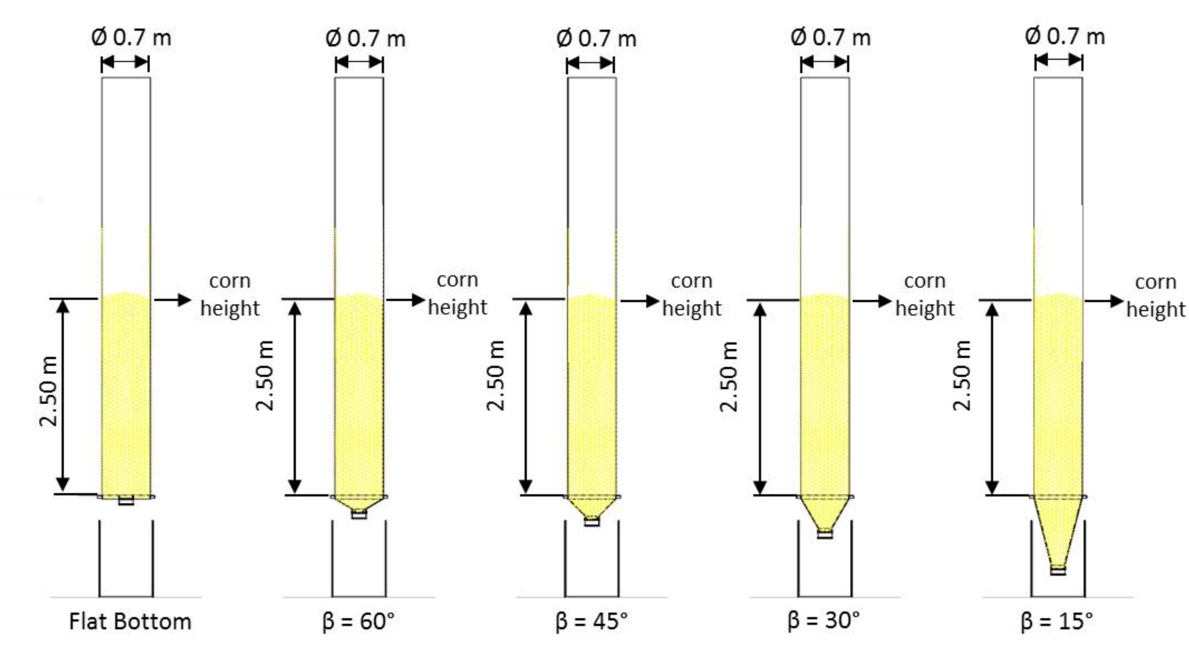

Figure 8. Test configuration, varying the hopper angle.

The reason of using this hopper inclinations was due to Eurocode 1, part 4. The inclinations of the hoppers associated with the friction coefficient of the wall with the product (μ) (in the case of this work smooth steel wall with maize) provide different flows (Figure 4). Mass flow for β = 15 °; transition flow for β = 30 ° and funnel flow for β = 45 and 60° and flat bottom. Therefore, it possible to study the flow during discharge.

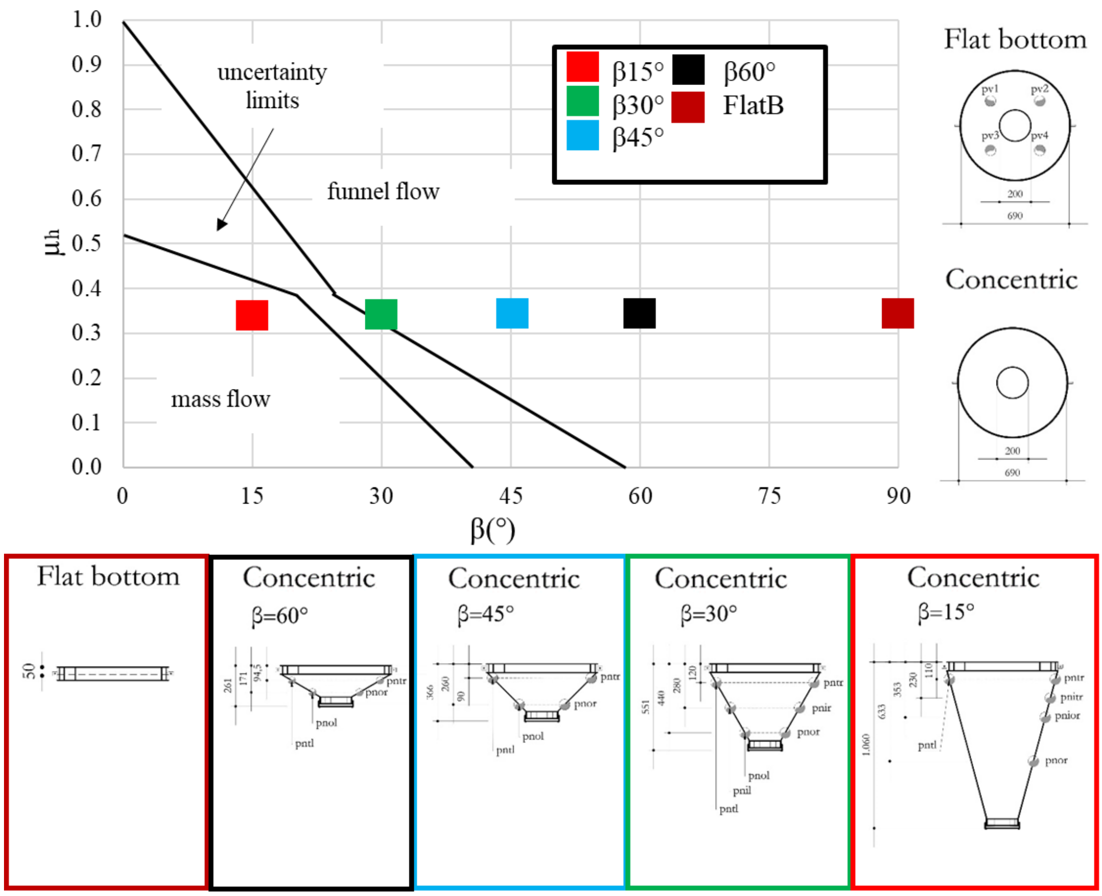

Figure 9. Hopper angles and conditions for flow patterns according to Eurocode 1, part 4.

Also, according to Eurocode, it was possible to distinguish the 5 different bottoms in three other groups regarding the type of silo: steep hopper, shallow hopper and flat bottom. Therefore, the bottoms were classified and calculated as follows:

- Flat bottom (FlatB) is a flat bottom because $\alpha < 5°$;
- $\beta = 60°$ is a shallow hopper because $\tan\beta > \frac{1-K}{2\mu_h}$;
- $\beta = 15°$; $\beta = 30°$ and $\beta = 45°$ are a steep hopper because $\tan\beta < \frac{1-K}{2\mu_h}$.

The pilot silo was filled at a constant speed, providing approximate flow rates for the tests (Table 1).

Table 1. Average flow for each test.

	$\bar{X}$ (kg/s)		σ (kg/s)	
Test	Filling	Discharge	Filling	Discharge
FlatB	4.1	20.2	0.1	0.5
β60°	4.4	20.0	0.1	0.2

β45°	4.6	22.3	0.3	0.2
β30°	5.0	24.2	0.5	0.9
β15°	4.5	31.4	0.1	0.2

$\bar{X}$: mean; σ: standard deviation

The silo was discharge with the gate (diameter of 0.20 m) 100% open. In addition, still in relation to Table 1, it can be seen that the discharge flow rate it is directly influenced by the hopper inclination (and type of flow), greater for hoppers with smaller β. In addition, in this model of the pilot silo it was observed that the discharge flow is at least 5 times greater than that of the filling.

As each of the five configurations had different volume (because the volume of each hopper), the product loading values were also different. Table 2 presents the values related to the load of the storage product of each configuration.

Table 2. Average load for each test.

Test	$\bar{X}$ (kN)	σ (kN)
FlatB	7.49	0.53
β60°	7.86	0.45
β45°	8.46	0.15
β30°	8.38	0.81
β15°	9.26	0.19

$\bar{X}$: mean; σ: standard deviation

It is noteworthy that the β30° (β = 30°) test had a mean value different from that expected and a standard deviation higher than the others. The reason is that of the 6 repetitions, two showed flaws in the filling, resulting in heights of the stored product below that of interest. It should be emphasized that the two repetitions were used for calculations of means and standard deviations, however in the analysis of the individual test (presented later) they were removed during the random choice.

All tests were conducted in three steps: filling the silo to the height of interest (verified by the tension load cell that shows the measurement in the semi-cylinder above the height of interest), static condition (for 10 min); product discharge (hopper gate 100% opened).

2.5.3 Description of the analyzes

The topics presented in results and discussions compared and discussed the different concentric hopper inclinations evaluating the load and pressures, which according to Eurocode 1 part 4 [7] in Figure 4 represents three flow patterns at discharge.

The analysis of the results and discussions were divided into: Temporal behavior of the test configurations; Normal pressures in the cylinder 0.25 m above the transition (p_{h1}); Normal pressures in the cylinder 0.75 m above the transition (p_{h2}); Friction pressures in the cylinder 0.25 m above the transition (p_{w1}); Vertical stress in the stored product at the transition (p_{vt}); Coefficient of lateral pressures (K); Normal pressure at transition (p_{nt}); Maximum normal pressures (p_h max); Maximum friction pressures (p_w max).

Temporal behavior of the test configurations presents the temporal behavior of all instrumentation during the complete test, aiming to reinforce the quality of data collection and instrumentation. In addition, it discusses the differences, in general, between the different inclinations of the bottoms

Normal pressures in the cylinder 0.25 m above the transition (p_{h1}), Normal pressures in the cylinder 0.75 m above the transition (p_{h2}) and Friction pressures in the cylinder 0.25 m above the transition (p_{w1}) present the most detailed behavior of pressures (normal and friction) in these locations. Aiming to evaluate mainly the moment and the magnitude of the maximum pressures and the influence by the inclination of the bottom associated with a flow channel and static material. In addition to comparing with Eurocode.

Coefficient of lateral pressures (K) presents the temporal behavior of the coefficient of lateral pressures, emphasizing the moment of discharge and comparing with the coefficient (K) calculated by Eurocode.

Normal pressure at transition (p_{nt}) details the pressure behavior slightly below the silo-bottom transition, comparing the test configurations and verifying the magnitude and moment of pressure occurrence.

Maximum normal pressures (p_h max) and Maximum friction pressures (p_w max) the curve of maximum pressures (friction and normal) is plotted for each configuration and compares with those calculated by Eurocode.

3. Results and discussion

This paper generated a large volume of data. Therefore, to avoid exposing unnecessary data, are presented the values of average and standard deviation in each measurement cell referring to filling and discharge (Table 4).

Table 4. Maximum mean values of pressures after filling and discharge in each test configuration.

After filling pressure (kPa)										
Cell	FlatB		β60°		β45°		β30°		β15°	
	$\bar{X}$	σ	$\bar{X}$	σ	$\bar{X}$	σ	$\bar{X}$	σ	$\bar{X}$	σ
p_{h5}	0.44	0.35	0.19	0.17	0.18	0.03	0.12	0.06	0.08	0.06
p_{h4}	1.96	0.51	1.21	0.15	0.69	0.07	0.75	0.24	0.74	0.02
p_{h3}	3.16	0.70	2.39	0.05	0.95	0.01	1.53	0.57	1.59	0.21
p_{h2}	3.76	0.21	2.54	0.25	0.96	0.05	1.28	0.07	1.14	0.25
p_{h1}	4.81	0.09	4.22	0.15	1.67	0.05	2.83	0.07	2.53	0.07
p_{nt}	-	-	2.06	0.12	1.99	0.42	1.71	0.10	4.30	0.46
p_{ni}	-	-	-	-	-	-	2.99	0.17	-	-
p_v	8.70	0.29	-	-	-	-	-	-	-	-
p_{nit}	-	-	-	-	-	-	-	-	3.72	0.51
p_{nio}	-	-	-	-	-	-	-	-	2.33	0.80
p_{no}	-	-	6.89	0.30	7.08	1.00	5.63	0.33	4.56	0.29
p_{vt}	10.77	0.43	9.87	1.94	9.38	0.47	11.53	0.76	9.91	0.79
p_{w5}	0.13	0.06	0.08	0.06	0.18	0.03	0.06	0.02	0.08	0.01
p_{w4}	0.43	0.11	0.56	0.16	0.69	0.07	0.30	0.22	0.45	0.05
p_{w3}	0.71	0.10	0.79	0.09	0.95	0.01	0.68	0.08	0.81	0.08

p_{w2}	0.94	0.10	0.89	0.10	0.96	0.05	0.69	0.14	0.84	0.05
p_{w1}	1.41	0.05	1.55	0.36	1.67	0.05	1.07	0.13	1.57	0.10
Discharge pressure (kPa)										
Cell	FlatB		β60°		β45°		β30°		β15°	
	$\bar{X}$	σ	$\bar{X}$	σ	$\bar{X}$	σ	$\bar{X}$	σ	$\bar{X}$	σ
p_{h5}	0.64	0.71	0.61	0.51	0.39	0.04	0.15	0.13	0.00	0.10
p_{h4}	3.21	0.59	3.33	0.28	0.99	0.04	2.53	0.73	2.74	0.13
p_{h3}	4.04	0.54	3.81	0.31	1.32	0.01	4.33	0.62	4.26	0.27
p_{h2}	3.68	0.14	4.71	0.22	1.29	0.02	4.41	0.11	4.63	0.40
p_{h1}	4.78	0.12	4.30	0.12	1.77	0.02	4.95	0.11	3.90	0.21
p_{nt}	-	-	13.20	1.10	13.12	1.18	15.89	1.68	26.08	2.05
p_{ni}	-	-	-	-	-	-	4.33	0.45	-	-
p_{v}	9.97	0.45	-	-	-	-	-	-	-	-
p_{nit}	-	-	-	-	-	-	-	-	10.11	1.97
p_{nio}	-	-	-	-	-	-	-	-	4.59	0.19
p_{no}	-	-	6.57	0.21	6.81	1.45	5.06	0.15	4.50	0.21
p_{vt}	10.56	0.48	7.43	0.70	8.32	0.33	10.88	0.71	8.21	1.34
p_{w5}	0.27	0.13	0.18	0.13	0.39	0.04	0.12	0.05	0.16	0.01
p_{w4}	0.77	0.18	0.76	0.23	0.99	0.04	0.44	0.36	0.66	0.05
p_{w3}	1.14	0.11	1.14	0.06	1.32	0.01	0.98	0.16	1.15	0.09
p_{w2}	1.08	0.08	1.03	0.11	1.29	0.02	1.15	0.07	1.18	0.08
p_{w1}	1.35	0.05	1.59	0.41	1.77	0.02	1.36	0.21	1.84	0.16

$\bar{X}$: mean value; σ: standard deviation

As noted, the tests showed little coefficient of variation. Therefore, for each type of test, one of the six repetitions were chosen randomly to discuss the results.

Temporal behavior of the test configurations

It can be seen that the model is accurate (Figure 5) showing the behavior of the measurement cells in the 15 pressure curves. The images refer to the five test configurations and the three divisions of the measurement cells. It is observed the equidistance of the normal pressures ($p_{h\ (1.5),\ t}$) and the linearity of the weight of the stored product (W).

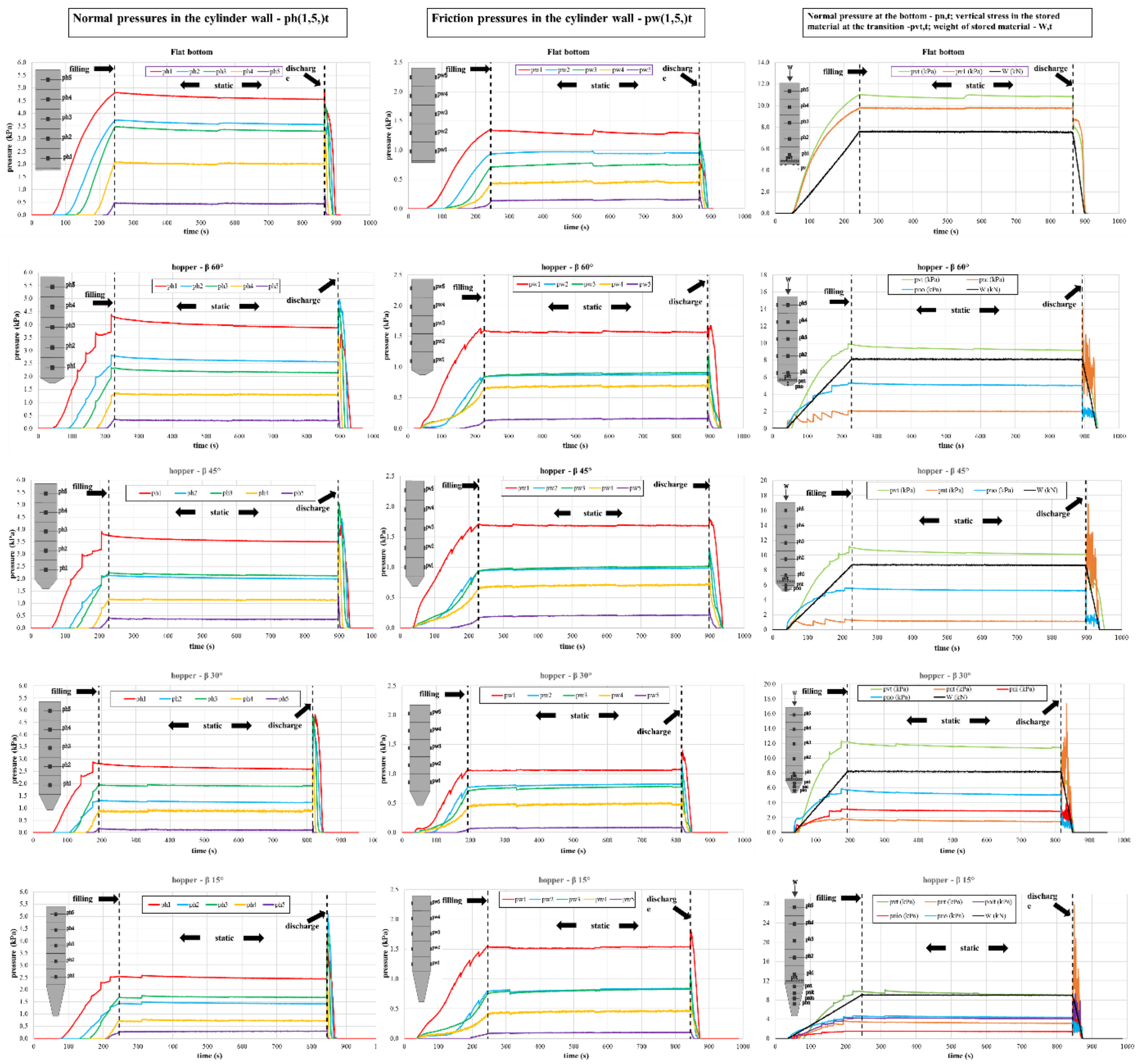

Figure 10. Normal silo cylinder wall pressures ($p_{h,t}$), friction silo cylinder wall pressures ($p_{w,t}$), normal hopper wall pressures ($p_{n,t}$), vertical stress in the stored product at the transition ($p_{vt,t}$) and weight of stored product ($W_{,t}$).

The flat bottom in the filling does not show settling peak due to the right angle (β = 90 °), providing stability of the stored product. Therefore, in the cylinder and bottom of the silo there are no oscillations in friction and normal pressures.

It is observed that between the height 0.75 and 1.25 meters (p_{h2} and p_{h3}), as the angle β decreases (β: 90, 60, 45, 30 and 15 °), the normal pressures in the cylinder tend to cross. At β = 45 ° they cross at the end of filling and at β = 30 and 15 ° they cross just after the start of filling. It is believed that the smaller the hopper angle, the greater the formation of mechanical arches between 0.75 and 1.25 m. Some authors have verified the same finding, however, using other stored products [27,48,50].

The friction pressures clearly show the settling peaks in all configurations, even if the stored product was only 10 minutes static, it is easy to see the peaks provided by the consolidation. This finding was verified for the first time in 2012 [48], however there are still many gaps in the prediction of this behavior.

Normal and friction pressures at discharge have greater magnitude according to the decrease in the hopper angle, in other words p_h, p_n and p_w β (90 <60 <45 <30 <15 °). In addition, the maximum normal pressures in the cylinder ($p_{h\ (1.5),\ t}$) are approximately 5 kPa, that is, during filling and static condition, the normal pressures in the cylinder are higher for larger β. However, at discharge the overpressure is greater in β less, but all have an approximate maximum value.

The normal pressures in p_{h1} and p_{h2} showed a significant variation due to the angle of β. It is believed that there is a static zone (flow channel) that changes according to the hopper angles and influences the behavior of pressures at 1/3 the height of the silo cylinder (0.83 m). Therefore we decided to analyze more carefully the temporal behavior of p_{h1} and p_{h2} in the five configurations.

Normal pressures in the cylinder 0.25 m above the transition (p_{h1})

The silo-hopper transition presents the maximum overpressures at discharge because the stored product changes from static to dynamic condition and the vertical displacement of the stored product in the geometric transition, for mass flow [5,51]. In the funnel flow there are stored product channels (effective transition), that is, static material forming a passage of the product to the outlet gate of the silo, dampening the pressures [23,45]. These theories and affirmations are seen in Figure 6 in a simple and visual way.

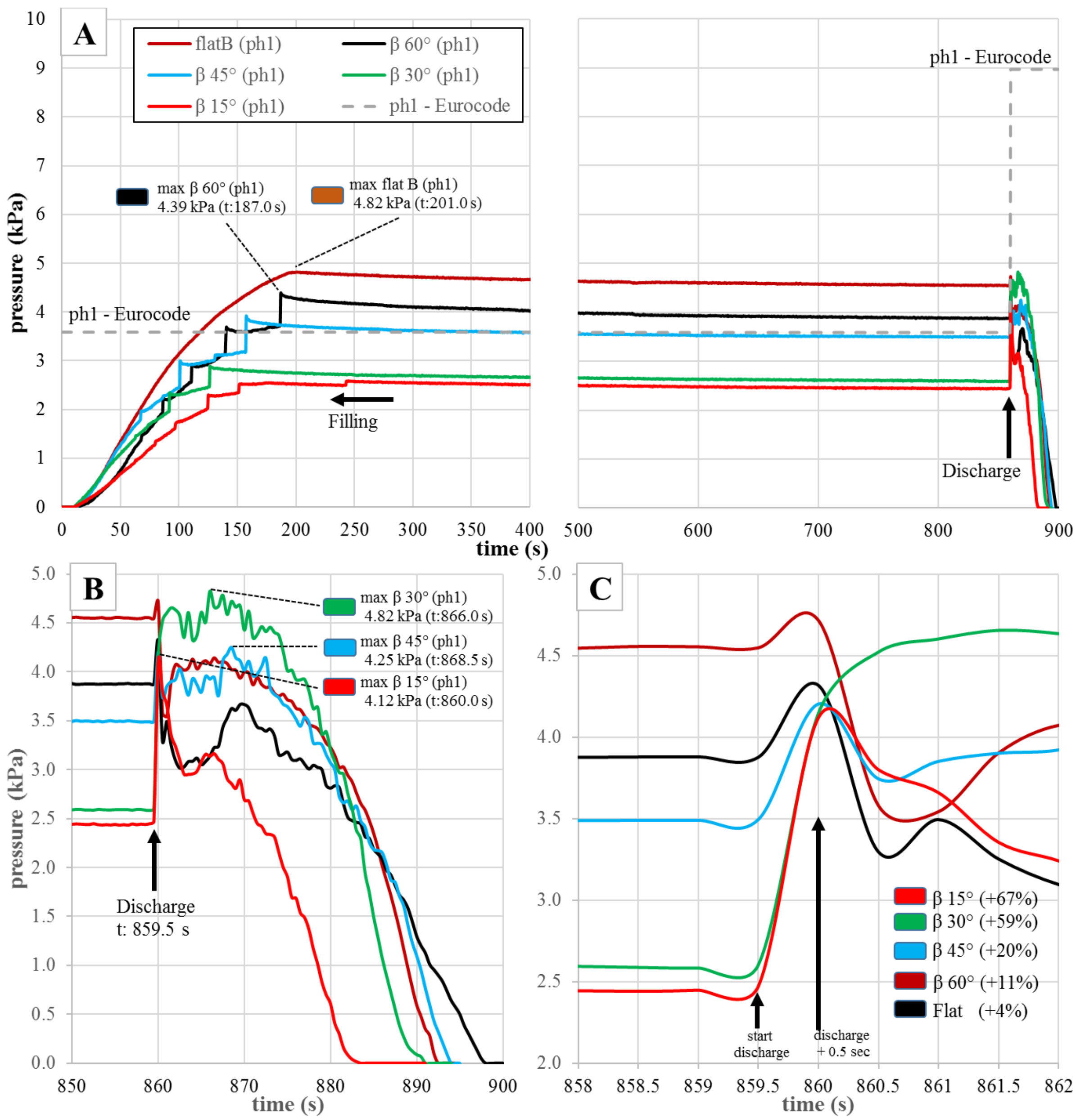

Figure 11. Normal pressures in the cylinder ($p_{h1,\,t}$) 0.25 m above the transition.

(A) Complete test; (B) Discharge; (C) Overpressures.

It is observed that in Figure 6A, during filling, the maximum normal pressures in the cylinder occurred for FlatB and β60 ° at height 0.25 m (p_{h1}). The flow pattern of the two configurations is funnel flow, and geometrically they are flat bottom (FlatB) and shallow hopper (β60 °) according to Eurocode.

Figure 6B demonstrated that for β45 °, β30 ° and β15 ° the maximum normal pressures in the cylinder occurred at discharge. Although, according to Eurocode, hoppers with funnel flow (β45 °), mixed flow (β30 °) and mass flow (β15 °) are geometrically steep type hoppers. Another interesting fact is the moment of occurrence after the discharge, first β15 ° followed by β30 ° and β45 °.

Exactly after the start of the discharge and 0.5 seconds before, the overpressure in p_{h1} was calculated for all configurations (Figure 6C). It was found that according to the greater angle in β, the lower the overpressure, that is, p_{h1} (β15 °> β30 °> β45 °> β60 °> FlatB). Figure 6A shows that the maximum experimental pressures are lower than that calculated by Eurocode.

In order to understand if increasing the height of the cylinder (0.75 m, p_{h2}) the normal pressures would be influenced by the formation of flow channel and static stored product according to the angle β, the same analysis was conducted.

Normal pressures in the cylinder 0.75 m above the transition (p_{h2})

During filling, the occurrence of the maximum normal pressure in the cylinder was verified in FlatB (Figure 7A), presenting values higher than those calculated by Eurocode.

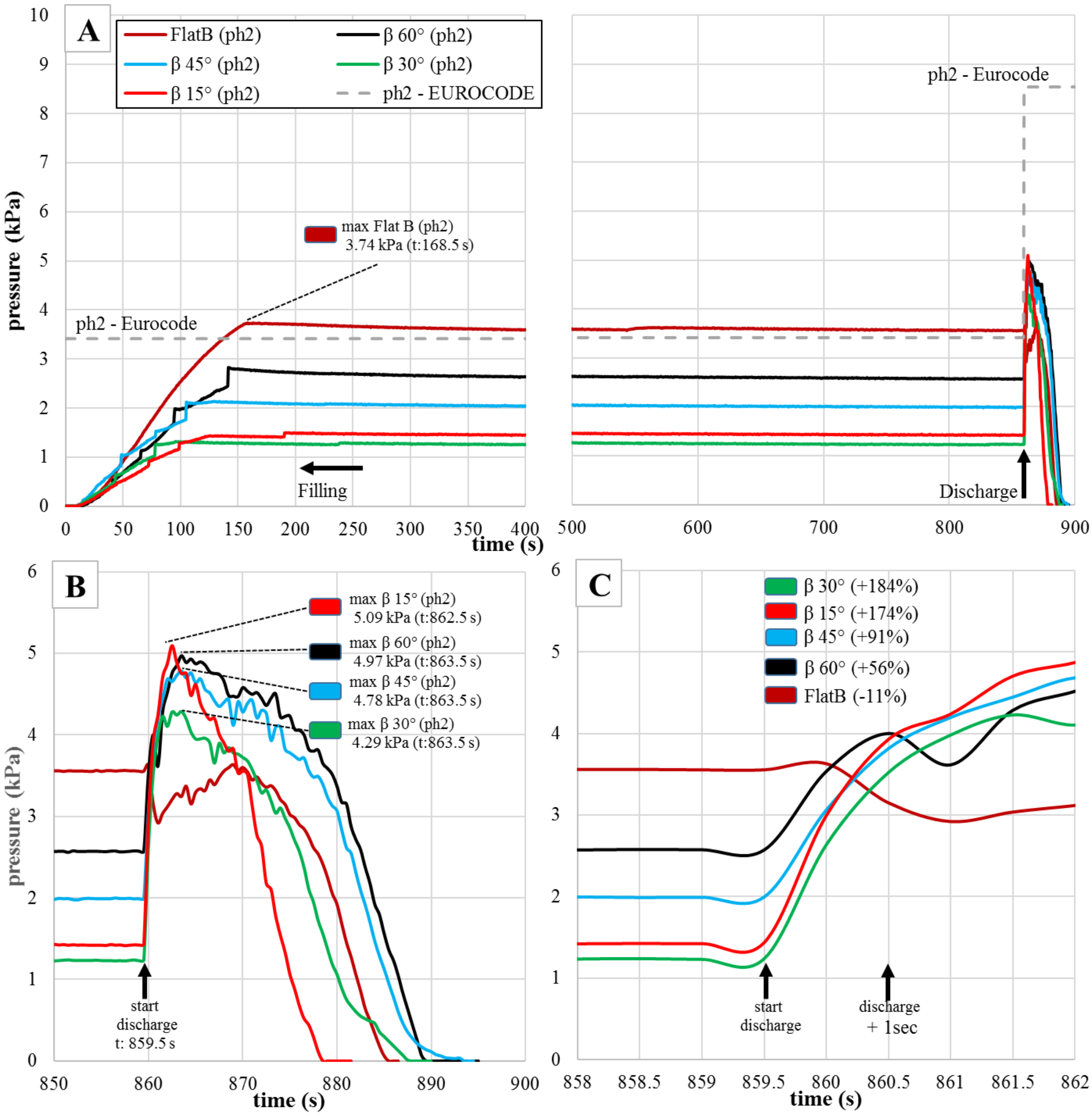

Figure 12. Normal pressures in the cylinder ($p_{h2,\,t}$) 0.75 m above the transition.

(A) Complete test; (B) Discharge; (C) Overpressures.

The maximum normal pressures in the cylinder at discharge (Figure 7B), once again, demonstrate that for mass flow (β15 °) it had the highest overpressure and occurred in the shortest time. Subsequently, those with funnel flow (β45 ° and β60 °) and mixed flow (β30 °). Comparing with Figure 6B, it can be seen that the overpressure at β30 ° decreased and for β45 ° and β60 ° increased, due to the greater height of the flow channel and because β30 ° is classified as a transition flow, influenced by the height of the stored product.

The overpressures (Figure 7C) shows that the highest was at β30 °, however, if we compare with Figure 6C ($p_{h1,}$ with 0,25 m) the increase in β45 ° and β60 ° was 3 to 4 times, while β15 ° and β30 ° was less than 2 times and in FlatB there have been no changes. In other words, affirming the pressure damping zones (static product zones) for hoppers with a greater β angle (effective transition). Checking the influence of the hopper type and the type of flow, at height 0.25 m the friction pressure in the cylinder (p_{w1}) was also evaluated.

Friction pressures in the cylinder 0.25 m above the transition (p_{w1})

As with normal cylinder pressure at 0.25 m (p_{h1}) (Figure 6A), the maximum friction pressure in FlatB occurred during filling (Figure 8A).

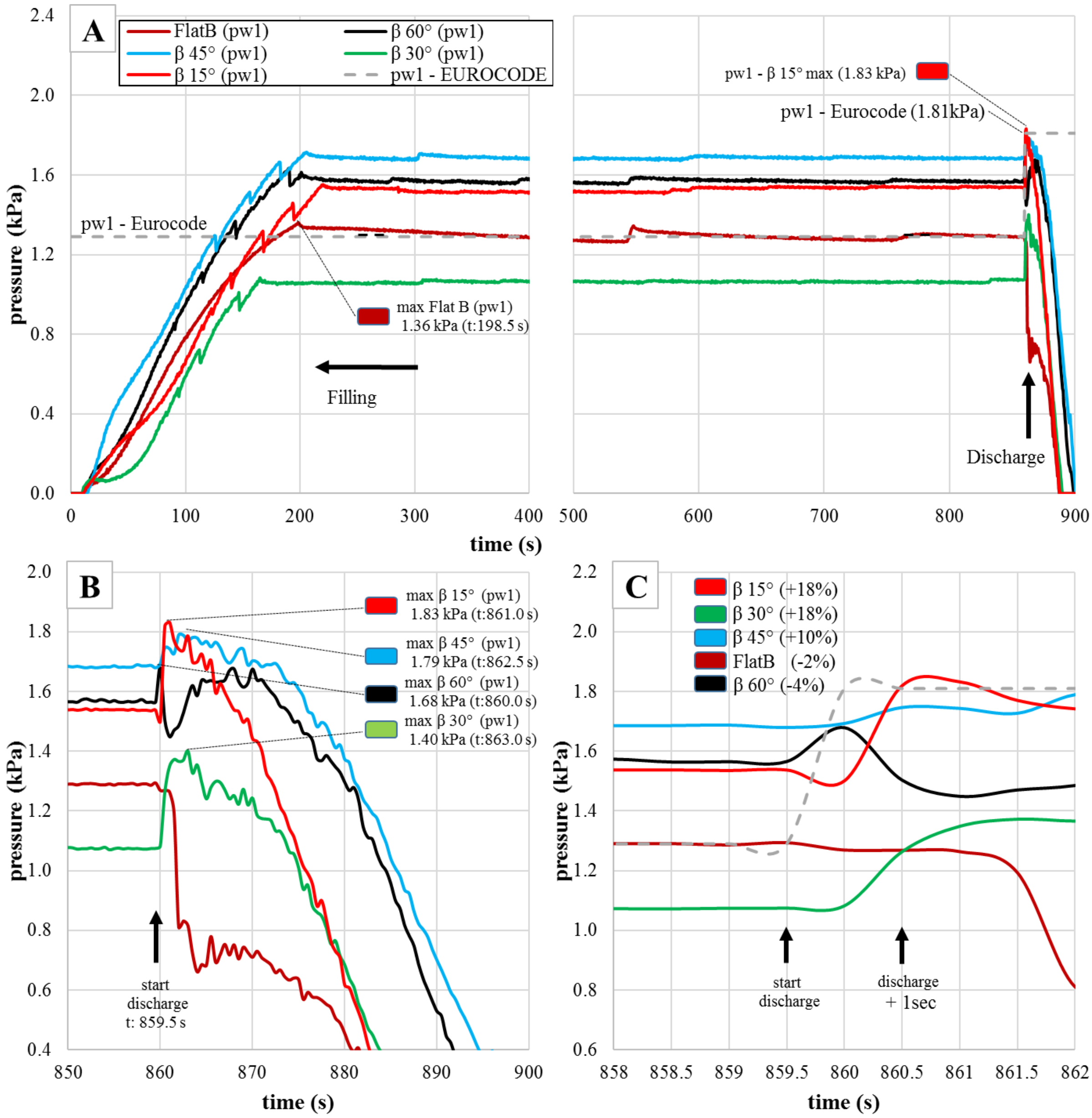

Figure 13. Friction pressures in the cylinder ($p_{w1,\,t}$) 0.25 m above the transition.
(A) Complete test; (B) Discharge; (C) Overpressures.

For funnel flow hoppers and classified as flat bottom (FlatB) and shallow hopper (β60 °), in the discharge, after a few seconds there was a sharp drop in pressure (Figure 8B). In FlatB it was due to the static material and at β60 ° possibly when emptying the hopper, the product was accommodated by increasing the pressure in a few seconds. For steep hoppers (β45 °, β30 ° and β15 °) peak pressure occurred at the beginning of the discharge.

The overpressures calculated after 1 second from the beginning of the discharge indicate that the magnitude is directly related to the decrease in β (Figure 8C). Only in FlatB that the stored product was static for two seconds before the pressure drop.

In general, it is observed that almost all configurations exceeded that calculated by Eurocode during filling, however, in the discharge, only at β15 ° was higher than the standard.

Coefficient of lateral pressures (K)

The Lateral pressure ratio (K) is obtained by Eurocode [7] in a simple way, only by the type of the stored product, not being influenced by the geometry of the hopper. Figure 10 presents the values during the tests performed in all configurations, being possible to evaluate the behavior of K in each one of them. The significant change in pressures (p_{vt} and p_{h1}) results in the values of the lateral pressure ratio (K), which is influenced by the angle β. (Figure 10).

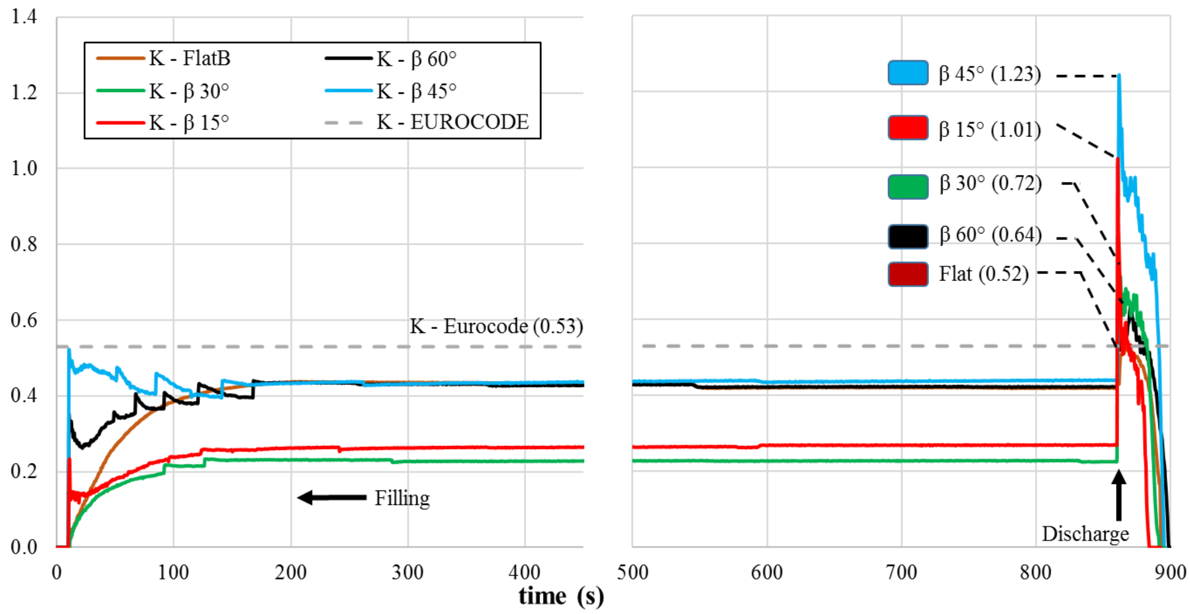

Figure 14. Temporal behavior of the coefficient of lateral pressures ($K_{,t}$) at transition.

It is observed that practically all configurations at discharge exceeded the K calculated by Eurocode, except for FlatB (flat bottom and funnel flow). The highest K was in β45 ° (steep hopper and funnel flow), later β15 ° (steep hopper and mass flow) and β30 ° (steep hopper and transition flow). The same was confirmed by some authors who noticed a considerable increase in K during the first seconds of the discharge surpassing Eurocode 1, part 4 [27,48,50].

Obviously, K increases when the discharge occurs, but it is interesting that for β45º it increases a lot, although it is not basic flow. Therefore, it is believed that because it is half the right angle (90 º) and because β45º has the lowest p_{vt} (Figure 5), providing the highest lateral pressures ratio in the transition between the 5 configurations.

Normal pressure at transition (p_{nt})

The normal pressures on the silo cylinder wall during discharge are erratic for mass flow [52]. In Figure 11 it is observed in the mass flow (β15 °), the pressures during the discharge oscillate considerably. Oscillations also occur in the funnel flow and transition flow (β60 °; β45 ° and β30 °), but with lesser magnitude and more normalized.

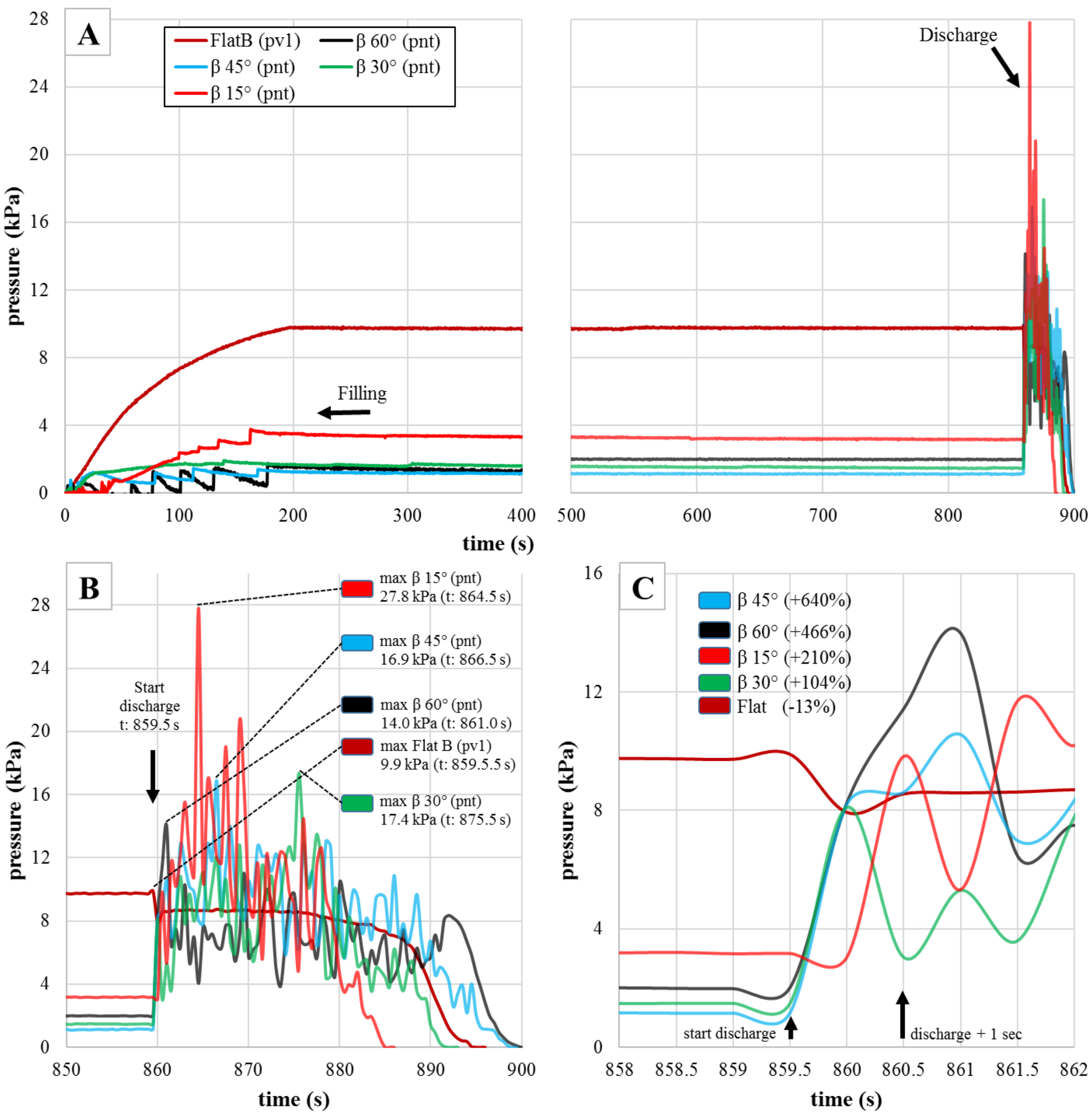

Figure 15. Normal pressures in the bottoms (hopper and flat) (pnt,t, pv1,t).

(A) Complete test; (B) Discharge; (C) Overpressures.

During filling, it is observed that (Figure 11A), opposite to the normal pressure in the cylinder above the transition (0.25 m, ph1) (Figure 6), and with the exception of the flat hopper (FlatB) the pressures are higher according to the decrease in β. It is also found that the settling peaks are higher at β60 ° and decrease until β15 °, with the exception of β30 °. Possibly, during filling, this point is a dead zone, where no acting forces are found due to the decrease of the β angle.

Maximum normal pressures (ph max)

The maximum pressure curves during filling and discharge are shown in Figure 12. The results were compared with those calculated by Eurocode 1, part 4 [7].

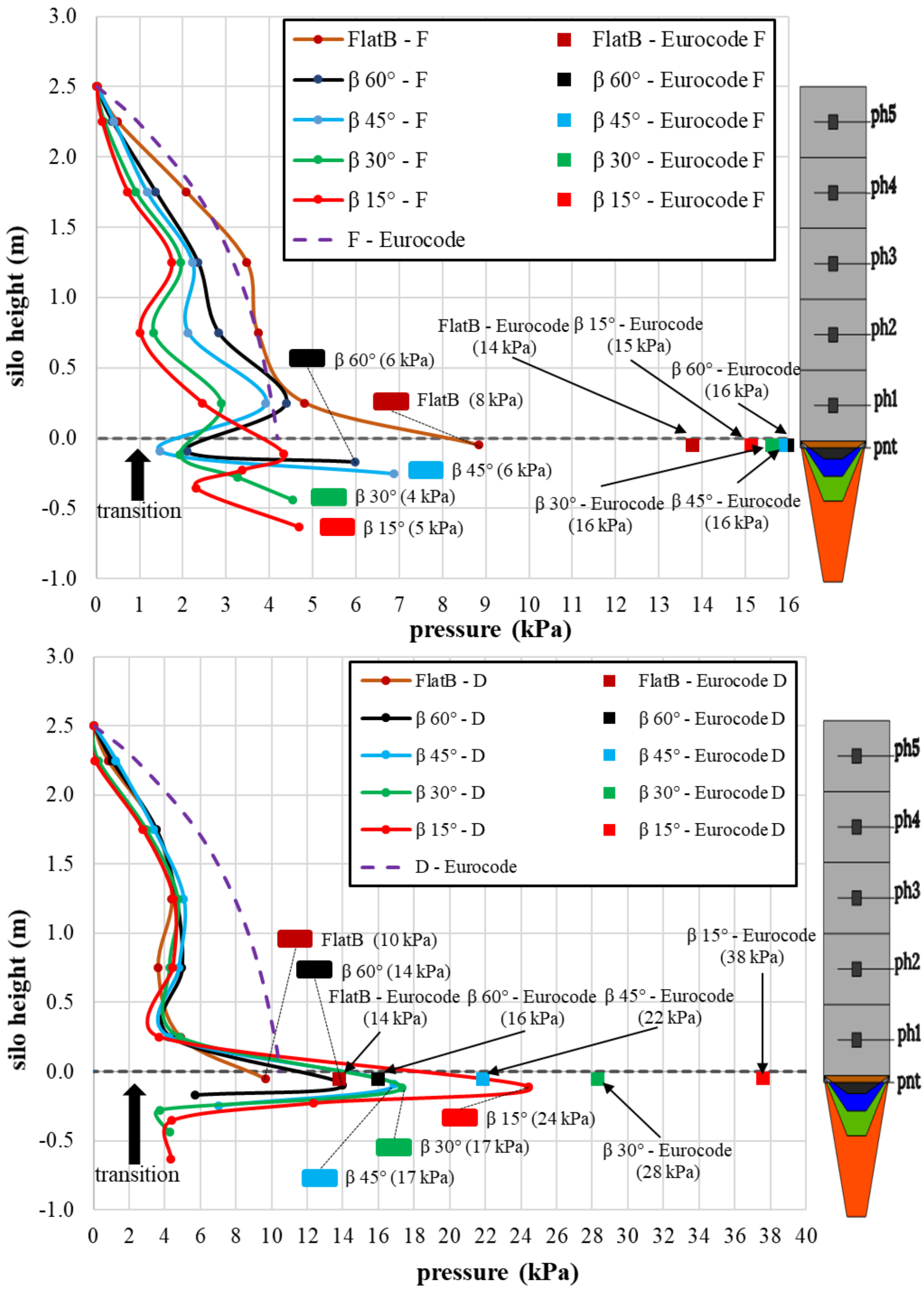

Figure 16. Maximum normal pressures on the wall (ph and pn). Comparison with Eurocode 1, part 4.

F: Filling; D: Discharge.

Observing the shapes of the discharge curves (Figure 12), it seems that for an angle of β15º we have a mass flow, however for the rest of the angles we have a channel flow. In the case of funnel flow the horizontal loads are lower just below the hopper, but on the vertical wall it will have a greater load, due to the fact that an interior hopper is formed through which the grain slides. In the funnel flow it is normal that at some point on the vertical wall it has greater pressures than those obtained for mass flow, they are surely located in an area near the transition of the internal hopper. It seems that β30 º, β45 º and β 60º have the maximum pressure on the vertical wall at a height of 1.25 m, but this is not exactly the case, it is because the measurement cells are at that height, is not possible to say what happens below or above. That is, the pressure can be higher between measurement cells. Although the result is not exact, it is very close to reality.

Differences between the filling and discharge curves depending on whether it is mass or funnel flow are also interesting, in the mass flow the pressures are high in p_{h1} for filling, but they do not grow as much as in p_{h3} during the discharge, for the effect we have previously indicated (inner cone). It is also interesting that there is less difference between filling and discharge when the bottom is flat.

The pressures obtained experimentally are lower when compared to the values obtained by Eurocode 1, part 4. Although during filling and near transition (p_{h1}) the values for hopper flow hoppers (, β45 º, β 60º and FlatB) are higher than the standard. However, this does not compromise the standard regarding silo design, as design calculations are made with discharge values and not filling values.

Maximum friction pressures (pw max)

Figure 13 gives the maximum frictional pressures in the cylinder compared with those given in Eurocode 1, part 4, showing the five configurations divided between the five hopper geometries.

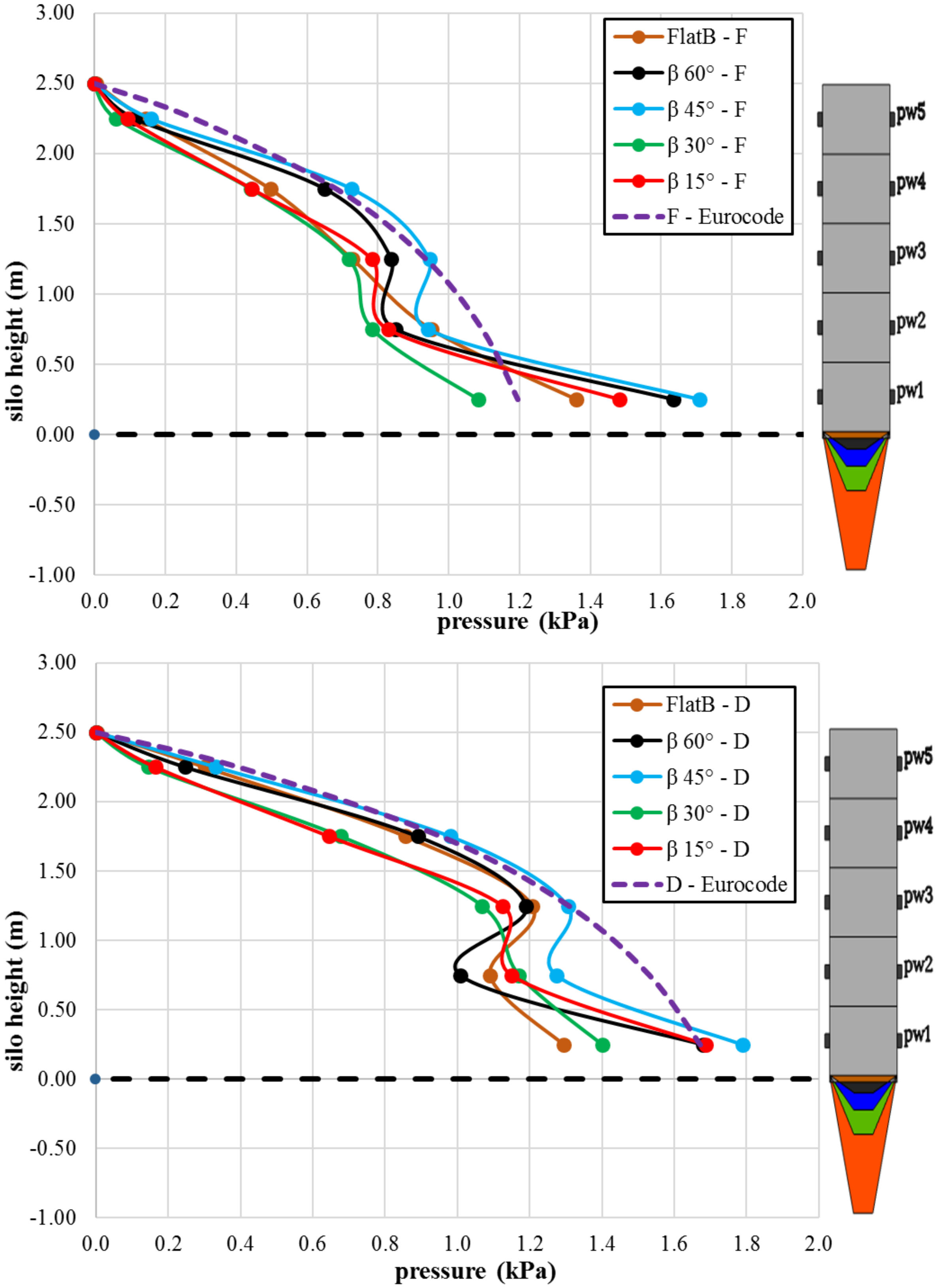

Figure 17. Maximum friction pressures on the wall (pw). Comparison with Eurocode 1, part 4.

F: Filling; D: Discharge.

The maximum experimental frictional pressures in the pilot silo exceeded those obtained by Eurocode 1, part 4 at several points. Several failures have occurred related to buckling due to the vertical force exerted on the wall of the silo in Brazil.

It was not possible to understand a pattern related to friction pressures with hopper angles. We observed that the β45 º hopper presented the highest pressure values regardless of the phase (filling or discharging). Furthermore, quantitatively, the values of friction pressures at the time of discharge did not show a significant increase.

It is interesting to say that for all variables (hopper angles and silo phases) a decrease in friction pressure was observed at 0.75 meters, corresponding to 1/3 of the total height of the silo.

We believe that the possible reason is because the Vertical stress in the stored product ($p_{vt,}$) at the transition (Figure 5) is the smallest among the hopper angles, providing the highest coefficient of lateral pressure (K), in other words, half the right angle, β = 45 °, provides the greatest destabilization of the stored product and increases the friction force on the silo wall. Even so, we can see in Figure 5 a, that in discharge, the $p_{vt,}$ for β45 ° presented the greatest drop in the vertical stress.

4. Conclusions

Flat bottom hoppers have a discharge flow greater than or equal to shallow hoppers (β = 60 °) when using maize.

During silo filling the flat bottom does not shows settling peaks.

The smaller the angle in β promotes a larger formation of stress arcs close to 1/3 of the height of the silo.

The moment of maximum normal pressures at 0.25 m above the transition is different in relation to the hopper angle. For flat bottom (β = 90 °) and shallow hoppers (β = 60 °) they occurred at the end of filling, for steep hoppers (β = 45 °; 30 °; 15 °) they occurred at the beginning of discharge.

Also, in relation to the normal pressures at 0.25 m above the transition (or 1/10 of silo height), the magnitude of the overpressures at the beginning of the discharge was directly proportional to the decrease in the hopper angle (β). In other words, the magnitudes of the overpressures were: β15 ° > β30 ° > β45 ° > β60 ° > β90 °.

Friction pressures at 0.25 m above the transition were higher than those obtained by Eurocode 1 part 4 during filling.

The coefficient of lateral pressures (K) at discharge exceeded that calculated by the standard for all hopper bottoms, except for the flat bottom.

Normal pressure between 1/10 to 1/3 of silo height vary considerably according to the hopper angle. The reason is that there is a static zone (flow channel) that varies according to the inclination of the bottoms.

Hoppers with a higher angle (in this case β = 90°) promote greater normal pressures on the cylinder wall during the filling and static phases. However, at discharge, the maximum pressures tended to coincide. Thus, overpressure during discharge using hoppers with a smaller angle (in this case β = 15°) was greater. In addition, the settling peaks and the magnitude of the pressure during settling rose as silo slenderness increased.

It is observed that several factors during discharge are out of the pattern due to the transition flow classification in β30 °, such as: the moment of occurrence of the maximum pressure in the transition, friction pressures 0.25 above the transition, normal pressures 0.25 and 0 .75 above transition, vertical stress in the stored product at the transition.

5. Declaration of Competing Interest

The authors declare that they have no known competing financial interests or personal relationships that could have appeared to influence the work reported in this paper.

6. Acknowledgements

The authors are very grateful to CAPES (Coordenação de Aperfeiçoamento de Pessoa de Nível Superior) for funding the doctoral scholarship related to the project.

REFERENCES

[1] H.A. Janssen, Versuche uber getreidedruck in silozellen, Z. Ver. Dtsch. Ing. 39 (1895) 1045–1049.

[2] D. Walker, An approximate theory for pressures and arching in hoppers., Chem. Eng. Sci. 22 (1967) 486. https://doi.org/10.1016/0009-2509(67)80145-3.

[3] J.K. Walters, A theoretical analysis of stresses in axially-symmetric hoppers and bunkers, Chem. Eng. Sci. 28 (1973) 779–789. https://doi.org/10.1016/0009-2509(77)80012-2.

[4] J.K. Walters, A theoretical analysis of stresses in silos with vertical walls, Chem. Sci. 28 (1973) 13–21.

[5] A.W. Jenike, J.R. Johanson, J.W. Carson, Bin loads—part 3: mass-flow bins, J. Manuf. Sci. Eng. Trans. ASME. 95 (1973) 6–12. https://doi.org/10.1115/1.3438163.

[6] DIN, DIN 1055-6: Basis of design and actions on structures – Part 6: design 623 loads for buildings and loads in silo bins, in: Berlin, Verlaz, 2005.

[7] CEN, EN 1991-4:2006. Eurocode 1: Actions on Structures. Part 4: Silos and Tanks, Brussels, 2006.

[8] A.. Jenike, Storage and Flow of Bulk Solids Bull. 123, University of Utah, 1964.

[9] WPMPS, Standart Shear Testing Technique for Particulate Solids Using the Jenike Shear Cell“, England, 1989.

[10] A. Dogangun, Z. Karaca, A. Durmus, H. Sezen, Cause of damage and failures in silo structures, J. Perform. Constr. Facil. 23 (2009) 65–71. https://doi.org/10.1061/(ASCE)0887-3828(2009)23:2(65).

[11] F. Ayuga, Some unresolved problems in the design of steel cylindrical silos., in: J.G. Chen, J.F., Teng (Ed.), Struct. Granul. Solids From Sci. Princ. to Eng. Appl., CRC Press-Taylor & Francis Group, Boca Raton, USA, 2008: pp. 123–133.

[12] J. Nielsen, From silo phenomena to load models, in: J.F. Chen, J.G. Teng (Eds.), Struct. Granul. Solids From Sci. Princ. to Eng. Appl., CRC Press-Taylor & Francis Group, Boca Raton, USA, 2008: pp. 49–57. https://doi.org/10.1201/9780203884447.

[13] CONAB - COMPANHIA NACIONAL DE ABASTECIMENTO, Acompanhamento da safra brasileira de grãos, Brasilia, 2022. https://www.conab.gov.br/component/k2/item/download/40788_0ee9dd05157257045355d00863c854b0.

[14] DPE - DIRETORIA DE PESQUISA E COORDENAÇÃO AGROPECUÁRIA, IBGE - Pesquisa de Estoques 2º semestre de 2019, 2019.

[15] Ministério da Agricultura Pesca y Alimentación, Avances de superficies y producciones agrícolas. Diciembre 2020, 2020.

[16] AGRICULTURA Y GANADERIA de Castilla y León, TABLAS DE LA COSECHA DE MAÍZ 2020 EN CASTILLA Y LEÓN, 2020. https://agriculturaganaderia.jcyl.es/web/jcyl/AgriculturaGanaderia/es/Plantilla100Detalle/1246464862173/Noticia/1284998741023/Recurso.

[17] J. Nielsen, Pressures from flowing granular solids in silos, Philos. Trans. R. Soc.

A Math. Phys. Eng. Sci. 356 (1998) 2667–2684. https://doi.org/10.1098/rsta.1998.0292.

[18] C. Bywalski, M. Kamiński, A case study of the collapse of the over-chamber reinforced concrete ceiling of a meal silo, Eng. Struct. 192 (2019) 103–112. https://doi.org/10.1016/j.engstruct.2019.04.100.

[19] Y. Sun, Y. Wang, Collapse reasons analysis of a large steel silo, Adv. Mater. Res. 368–373 (2012) 647–650. https://doi.org/10.4028/www.scientific.net/AMR.368-373.647.

[20] G. Gutiérrez, C. Colonnello, P. Boltenhagen, J.R. Darias, R. Peralta-Fabi, F. Brau, E. Clément, Silo collapse under granular discharge, Phys. Rev. Lett. 114 (2015) 5–9. https://doi.org/10.1103/PhysRevLett.114.018001.

[21] B.J. Teng, PLASTIC COLLAPSE AT LAP JOINTS IN PRESSURIZED CYLINDERS UNDER AXIAL LOAD, 120 (1994) 23–45.

[22] J.G. Teng, J.M. Rotter, Plastic collapse of restrained steel silo hoppers, J. Constr. Steel Res. 14 (1989) 139–158. https://doi.org/10.1016/0143-974X(89)90020-5.

[23] A.W. Jenike, J.R. Johanson, J.W. Carson, Bin Loads—Part 4: Funnel-Flow Bins, J. Eng. Ind. 95 (1973) 13–20.

[24] E.J. Benink, Flow and stress analysis of cohesionless bulk materials in silos related to codes, University of Twente, 1989.

[25] Internacional Organization for Standardization, ISO 11697:2012. Bases for design of strutures - Loads due to bulk materials, 2012.

[26] R.M. Gandia, F.C. Gomes, W.C. de Paula, P.J.R. Aguado, Influence of specific weight and wall friction coefficient on normal pressures in silos using the Finite Element Method, Rev. Eng. Na Agric. - Reveng. 29 (2021) 192–203. https://doi.org/10.13083/reveng.v29i1.12336.

[27] A. Couto, A. Ruiz, P.J. Aguado, Experimental study of the pressures exerted by wheat stored in slender cylindrical silos, varying the flow rate of material during discharge. Comparison with Eurocode 1 part 4, Powder Technol. 237 (2013) 450–467. https://doi.org/10.1016/j.powtec.2012.12.030.

[28] J.F. Chen, J.M. Rotter, J.Y. Ooi, Z. Zhong, Correlation between the flow pattern and wall pressures in a full scale experimental silo, Eng. Struct. 29 (2007) 2308–2320. https://doi.org/10.1016/j.engstruct.2006.11.011.

[29] A.J. Sadowski, J.M. Rotter, Structural Behavior of Thin-Walled Metal Silos Subject to Different Flow Channel Sizes under Eccentric Discharge Pressures, J. Struct. Eng. 138 (2012) 922–931. https://doi.org/10.1061/(asce)st.1943-541x.0000530.

[30] K. PIEPER, M. SCHÜTZ, Bericht Über das Forschungsvorhaben - Norm-Mess-Silo für Schüttguteigenschaften, Technische Universität Braunschweig, 1980.

[31] J. Zegzulka, The angle of internal friction as a measure of work loss in granular material flow, Powder Technol. 233 (2013) 347–353. https://doi.org/10.1016/j.powtec.2012.06.047.

[32] C.Y. Song, J.G. Teng, Buckling of circular steel silos subject to code-specified eccentric discharge pressures, Eng. Struct. 25 (2003) 1397–1417. https://doi.org/10.1016/S0141-0296(03)00105-6.

[33] C.J. Brown, J. Nielsen, Silos: Fundamentals of theory, behaviour and design, London, 1998.

[34] J.C. Calil, A.B. Cheung, Silos: pressões, fluxo, recomendações para o projeto e exemplo de cálculo, São Carlos, 2007.

[35] R.M. Gandia, F.C. Gomes, W.C. de Paula, E.A. de Oliveira Junior, P.J. Aguado Rodriguez, Static and dynamic pressure measurements of maize grain in silos

under different conditions, Biosyst. Eng. 209 (2021) 180–199. https://doi.org/10.1016/j.biosystemseng.2021.07.001.

[36] J.G. Teng, Y. Zhao, L. Lam, Techniques for buckling experiments on steel silo transition junctions, Thin-Walled Struct. 39 (2001) 685–707. https://doi.org/10.1016/S0263-8231(01)00030-1.

[37] A. Couto, A. Ruiz, P.J. Aguado, Design and instrumentation of a mid-size test station for measuring static and dynamic pressures in silos under different conditions - Part I: Description, Comput. Electron. Agric. 85 (2012) 164–173. https://doi.org/10.1016/j.compag.2012.04.009.

[38] W. Sun, J. Zhu, X. Zhang, C. Wang, L. Wang, J. Feng, Multi-scale experimental study on filling and discharge of squat silos with aboveground conveying channels, J. Stored Prod. Res. 88 (2020) 101679. https://doi.org/10.1016/j.jspr.2020.101679.

[39] C. V Schwab, I.J. Ross, G.M. White, D.G. Colliver, WHEAT LOADS AND VERTICAL PRESSURE, 37 (1994) 1613–1619.

[40] C.J. Brown, E.H. Lahlouh, J.M. Rotter, Experiments on a square planform steel silo, Chem. Eng. Sci. 55 (2000) 4399–4413. https://doi.org/10.1016/S0009-2509(99)00574-6.

[41] T. Schuricht, C. Furll, G.G. Eenstad, Full scale silo tests and numerical simulations of the „cone in cone” concept for mass flow, in: Handb. Powder Technol., Elsevier Science BV, 2001: pp. 175–180.

[42] Z. Zhong, J.Y. Ooi, J.M. Rotter, The sensitivity of silo flow and wall stresses to filling method, Eng. Struct. 23 (2001) 756–767. https://doi.org/10.1016/S0141-0296(00)00099-7.

[43] Y. Zhao, J.G. Teng, Buckling experiments on steel silo transition junctions. II:

Finite element modeling, J. Constr. Steel Res. 60 (2004) 1803–1823. https://doi.org/10.1016/j.jcsr.2004.05.001.

[44] J.G. Teng, X. Lin, Fabrication of small models of large cylinders with extensive welding for buckling experiments, Thin-Walled Struct. 43 (2005) 1091–1114. https://doi.org/10.1016/j.tws.2004.11.006.

[45] J. Härtl, J.Y. Ooi, J.M. Rotter, M. Wojcik, S. Ding, G.G. Enstad, The influence of a cone-in-cone insert on flow pattern and wall pressure in a full-scale silo, Chem. Eng. Res. Des. 86 (2008) 370–378. https://doi.org/10.1016/j.cherd.2007.07.001.

[46] A. Ramírez, J. Nielsen, F. Ayuga, On the use of plate-type normal pressure cells in silos. Part 1: Calibration and evaluation, Comput. Electron. Agric. 71 (2010) 71–76. https://doi.org/10.1016/j.compag.2009.12.004.

[47] A. Ramírez, J. Nielsen, F. Ayuga, On the use of plate-type normal pressure cells in silos. Part 2: Validation for pressure measurements, Comput. Electron. Agric. 71 (2010) 64–70. https://doi.org/10.1016/j.compag.2009.12.005.

[48] A. Ruiz, A. Couto, P.J. Aguado, Design and instrumentation of a mid-size test station for measuring static and dynamic pressures in silos under different conditions - Part II: Construction and validation, Comput. Electron. Agric. 85 (2012) 174–187. https://doi.org/10.1016/j.compag.2012.04.008.

[49] R.M. Gandia, F.C. Gomes, W.C. de Paula, E.A. de O. Junior, P.J.A. Rodriguez, Static and dynamic pressure measurements of maize grain in silos under different conditions, Biosyst. Eng. 209 (2021) 180–199. https://doi.org/10.1016/j.biosystemseng.2021.07.001.

[50] A. Couto, A. Ruiz, L. Herráez, J. Moran, P.J. Aguado, Measuring pressures in a slender cylindrical silo for storing maize. Filling, static state and discharge with different material flow rates and comparison with Eurocode 1 part 4, Comput.

Electron. Agric. 96 (2013) 40–56. https://doi.org/10.1016/j.compag.2013.04.011.

[51] M. Wójcik, J. Tejchman, G.G. Enstad, Confined granular flow in silos with inserts - Full-scale experiments, Powder Technol. 222 (2012) 15–36. https://doi.org/10.1016/j.powtec.2012.01.031.

[52] A.J. Sadowski, J.M. Rotter, Buckling of very slender metal silos under eccentric discharge, Eng. Struct. 33 (2011) 1187–1194. https://doi.org/10.1016/j.engstruct.2010.12.040.

Final considerations

The experimental station obtained new and unprecedented conclusions such as:

- normal pressure and friction relationships with consolidation;
- maximum silo pressure time at the beginning of discharge;
- pressure relationships with; consolidation; the discharge time by type of flow; influence of flow type on discharge pressures.
- Influence of slenderness in relation to K and Pvt.